



**PROGRAMA DE PÓS-GRADUAÇÃO EM OCEANOGRAFIA AMBIENTAL
UNIVERSIDADE FEDERAL DO ESPÍRITO SANTO**

UNIVERSIDADE FEDERAL DO ESPÍRITO SANTO
CENTRO DE CIÊNCIAS HUMANAS E NATURAIS
PROGRAMA DE PÓS-GRADUAÇÃO EM OCEANOGRAFIA AMBIENTAL

ALVARO E. S. SOARES

GEOACOUSTIC METHODS IN PORT AREAS: A MULTIFREQUENCY APPROACH.

Métodos Geoacústicos em Ambientes Portuários:
Uma Abordagem Multifrequencial.

VITÓRIA, 2019

ALVARO E. S. SOARES

GEOACOUSTIC METHODS IN PORT AREAS:
A MULTIFREQUENCY APPROACH.

Métodos Geoacústicos em Ambientes Portuários:
Uma Abordagem Multifrequencial.

Dissertação apresentada ao Programa de Pós-Graduação em Oceanografia Ambiental da Universidade Federal do Espírito Santo, como requisito parcial para obtenção do título de Mestre em Oceanografia Ambiental.

Orientador: Prof. Dr. Alex Cardoso Bastos
Co-orientadora: Prof. Dra. Valéria da Silva Quaresma.

Vitória, 2019.

ALVARO E. S. SOARES

GEOACOUSTIC METHODS IN PORT AREAS: A MULTIFREQUENCY APPROACH

Dissertação apresentada ao Programa de Pós-Graduação em Oceanografia Ambiental da Universidade Federal do Espírito Santo, como requisito parcial para obtenção do título de Mestre em Oceanografia Ambiental.

COMISSÃO EXAMINADORA

Prof. Dr. Alex Cardoso Bastos – Orientador
Universidade Federal do Espírito Santo / UFES

Prof. Dr. Fabian Sá
Universidade Federal do Espírito Santo / UFES

Prof. Dr. Luíz Antônio Pereira de Souza
Instituto de Pesquisas Tecnológicas de São Paulo / IPT



ATA DA 91ª SESSÃO PÚBLICA DE DEFESA DE DISSERTAÇÃO DE MESTRADO PELO ALUNO ALVARO EDUARDO SILVA SOARES

Às 09:00 horas do dia 25 do mês de março do ano de 2019, no Auditório IC2 do CCHN na UFES, Goiabeiras – Vitória (ES), reuniu-se a Banca Examinadora composta pelos professores Dr. Alex Cardoso Bastos (PPGOAm – Orientador), Dr. Fabian Sá (UFES) e pelo Dr. Luiz Antonio Pereira de Souza (IPT) para a sessão pública de defesa da dissertação do mestrando **Alvaro Eduardo Silva Soares**, com o título: **“MÉTODOS GEOACÚSTICOS EM AMBIENTES PORTUÁRIOS: UMA ABORDAGEM MULTIFREQUÊNICAL”**. Presentes os membros da banca e o examinando, o presidente deu início à sessão, passando a palavra ao aluno para sua exposição oral pelo intervalo de até 45 minutos. Posteriormente os membros da banca formularam as suas arguições, as quais foram respondidas pelo aluno. Em seguida, o presidente da sessão solicitou que os presentes deixassem a sala para que a banca pudesse deliberar; ao final das deliberações, o presidente da sessão convocou o mestrando e os interessados para ingressarem na sala; com a palavra, o presidente da banca leu a decisão da banca que resultou na **APROVAÇÃO** do examinando. A dissertação foi aprovada sem modificação de conteúdo. Por fim, o presidente da sessão informou que o aprovado somente poderá solicitar o Grau de Mestre após 1) *comprovar* o aceite de um artigo referente à sua dissertação, Qualis B2 ou superior, de acordo com o Comitê de Área da Capes onde o PPGOAM estiver sendo avaliado e 2) entregar a versão final de sua dissertação, em papel e meio digital, à Secretária do Programa devidamente aprovada pelo orientador. Nada mais havendo, foi encerrada a sessão da qual se lavra a presente ata, que vai assinada pelos membros da banca examinadora e pelo mestrando.

Prof. Dr. Alex Cardoso Bastos (Professor Orientador)

Prof. Dr. Fabian Sá (UFES)

Dr. Luiz Antonio Pereira de Souza (IPT)

Mestrando Alvaro Eduardo Silva Soares

ACKNOWLEDGMENTS

The author was granted a scholarship awarded by *Fundação de Amparo à Pesquisa do Estado do Espírito Santo* (FAPES). This research was supported by the *FAPES/VALE/FAPERJ Nº 01/2015 – Pelotização, Meio Ambiente e Logística* call. The Laboratory of Geological Oceanography and the Departamento de Oceanografia Geológica of the Universidade Federal do Espírito Santo provided technical equipment and processing tools.

Special thanks to:

Alex Bastos, my advisor, who granted me great opportunities, guidance and confidence during the development of this work and for the many insightful teachings;

Valeria Quaresma, my co-advisor, who was fundamental for my development as an academic student and for all the guidance and trust;

Souza, L.A.P (IPT, *Instituto de Pesquisas Técnicas – São Paulo*) for the technical support, guidance and promptitude during the geophysical survey. We also thank the technical support of the Cohesive Sediment Dynamics Laboratory LDSC/COPPE/UFRJ (*Universidade Federal do Rio de Janeiro*) in the person of Fonseca, D.L who assisted us with the densitometer survey and processing.

Thanks to the Examination Board for the availability, patience and kind constructive criticism.

Thank you, family, friends and Labogeo team, who are always there with support in all sort of matters.

ABSTRACT

Geophysical methods are a set of indirect methods of investigation that have great relevance in the study of submerged areas and stand out from conventional methods. These methods allow easy access to the areas of research and continuous observation of the surface and subsurface along a profile. Geoacoustic investigation utilizes the physical principle of elastic wave propagation to investigate the seafloor morphology and subsurface layer thicknesses.

In port regions, acoustic methods are widely applied for the determination of risks to marine navigation and dredging. Dredging projects are extremely costly and are potentially environmentally hazardous due to resuspension of contaminated materials and disruption of seabed conditions. Thus, single and multibeam bathymetry, seismic, sonographic and densitometric surveys are common activities for solving these and other issues. The acoustic signal backscatter pattern, obtained from these methods can be organized into groups and used for seabed mapping and sedimentological classification.

The state of *Espírito Santo* has national prominence in logistics with its ports, notably the Vale's Port of *Tubarão*. The maintenance of the navigation channels has always been a concern for the company, for the Brazilian navy, local authorities as well as the local communities.

Maritime ports generate a huge demand for resources, in addition to a series of environmental and social matters. Therefore it is of great importance to produce studies and techniques to map and identify the bottom and sub-bottom with both resolution and accuracy. The following questions are: what is the behavior of the different frequencies used on the most appropriate acoustic methods to map the sediment thickness in a navigation channel and what are the risks to navigation and dredging presented by defining such characteristics from these methods.

These questions are answered through the study of the acoustic methods with a multifrequency approach to map the bottom and sub-bottom of the port areas, and the analysis of the signal response produced by these methods.

In this project, acoustic techniques were used aiming at defining the best strategy and acoustic frequencies to be applied in maritime port terminals to solve questions concerning: nautical depth analysis, navigation risk assessment and the definition of the factual depth required for maintenance dredging. Acoustic multi frequency data and bottom unconsolidated density values were collected in order to respond to the abovementioned scientific questions.

Keywords: *geoacoustics, multifrequency approach, seismic, sonography, densitometry, ports, dredging, nautical depth.*

RESUMO

Métodos geofísicos são um conjunto de métodos indiretos de investigação que têm grande relevância no estudo de áreas submersas e se destacam dos métodos convencionais, pois possibilitam fácil acesso aos locais de interesse e permitem a observação contínua de estratos geológicos ao longo de um perfil. Investigações geoacústicas utilizam o princípio físico da propagação de ondas elásticas para investigar a morfologia de fundo e espessuras de camadas em subsuperfície.

Em regiões portuárias, métodos acústicos são extensamente aplicados para a determinação de riscos à navegação e dragagem. Obras de dragagem são extremamente onerosas e podem trazer consequências ambientais pela ressuspensão de materiais contaminados e perturbação das condições de sedimentação. Dessa forma, levantamentos batimétricos mono e multifeixe, sísmicos, sonográficos e densimétricos são atividades comuns para resolução destas e outras questões. O padrão de *backscatter* do sinal acústico, obtido a partir destes métodos pode ser organizado em grupos e utilizados para mapear o fundo marinho e para classificação sedimentológica.

O Espírito Santo tem destaque nacional em logística com seus portos de grande dimensão, nomeadamente o Porto de Tubarão da empresa Vale. A manutenção dos canais de navegação sempre foi uma preocupação da empresa, bem como para a marinha e para os locais onde esses portos estão localizados.

Uma obra desse tamanho gera uma enorme demanda de recursos, além de uma série de questões ambientais e sociais, dessa forma, é de grande importância produzir estudos e técnicas que mapeiem e identifiquem o fundo e subfundo de regiões portuárias com qualidade. Os questionamentos que se seguem são: qual o comportamento das diferentes frequências empregadas nos métodos acústicos e mais adequadas para mapear a espessura sedimentar em um canal de navegação e quais são os riscos à navegação e dragagem apresentados por definir tais características a partir destes métodos.

Esses questionamentos são respondidos através da aplicação de métodos acústicos com abordagem multifrequência no mapeamento de fundo e subfundo dos ambientes portuários e da análise da resposta do sinal produzido por esses métodos.

Neste aplicou-se técnicas acústicas para imagear o fundo e o subfundo marinho, visando definir a melhor estratégia e frequências a serem aplicadas em terminais portuários para questões que concernem a análise da profundidade náutica, avaliação do risco à navegação e confiabilidade da resposta do sinal acústico que correspondam à real profundidade que exige em dragagens de manutenção. Dados de multifrequência acústica e de densidade do material de fundo foram coletados, assim como buscou-se produzir uma classificação sedimentológica de superfície marinha e a proposta de análise integrada destes *dados a fim de justificar os usos e cuidados com cada técnica*.

Palavras-chave: *geoacústica, abordagem multifrequencial, sísmica, sonografia, densimetria, portos, dragagem, profundidade náutica.*

LIST OF TABLES

CHAPTER 1

Table 1 - Dimensions of the Port of *Tubarão*. (p. 14)

CHAPTER 3

Table 1 - Sediment content. (p. 34)

Table 2 - Correlation between geophysical and *in-situ* data. (p. 42)

Table 3- Penetration comparison, in percentage, of each source considering consolidated subsurface material. (p. 45)

Table 4 - Evaluation of the penetration and resolution for all frequencies according to each geological material. P stands for penetration and R for resolution (p. 49)

CHAPTER 4

Table 1 - R^2 obtained by the linear correlation between the depths found for the SBES 33kHz frequency and the corresponding depths for the volumetric mass density of 1150, 1175, 1200, 1225, 1250 kg/m³. (p. 67)

LIST OF FIGURES

CHAPTER 1

Figure 1 - Satellite image of the Port of *Tubarão*. The continuous black line expresses navigation channel and evolution basin. (p. 13)

CHAPTER 2

Figure 1 - Elastic deformation and particle motion. a) Primary Wave b) Secondary Wave, Telford et al. (1990). (p. 18)

Figure 2 - Elastic deformation and particle motion. a) Rayleigh b) Love waves. Bolt (1982). (p. 19)

Figure 3 - Snell's Law for reflection and refraction. Telford (1976). (p. 19)

Figure 4 - Relation between waveform and frequency. (p. 20)

Figure 5 - Environment investigation and suggested sources. Modified from Souza (2013). (p. 21)

Figure 6 - Comparison of the expected penetration between the sources Boomer and Sparker. Modified from <<http://www.geoacoustics.com>> November/2018. (p. 23)

Figure 7 - Sidescan sonar acquisition geometry. Modified from Mazel (1985). (p. 24)

Figure 8 - Reflection and backscattering by the SSS. Modified from Mazel (1985). (p. 24)

Figure 9 - Singlebeam echosounder operation. (p. 25)

Figure 10 - Combined nautical depth survey scheme. Modified from Fontein & Byrd (2007). (p. 26)

CHAPTER 3

Figure 1 - Localization of the evolution basin, access channel, surveyed lines and collected seabed material. (p. 32)

Figure 2 - Multifrequency seismic surveyed profiles on the access channel. a) HF Chirp, b) LF Chirp, c) Boomer, d) Processed Boomer. (p. 35)

Figure 3 - HF SSS surveyed line on the evolution basin. (p. 36)

Figure 4 - Multifrequency seismic surveyed profiles on the evolution basin. a) HF Chirp, b) LF Chirp, c) Boomer, d) Processed Boomer. (p. 37)

Figure 5 - Multifrequency seismic surveyed profiles on the access channel showing the crystalline basement outcrop. a) HF Chirp, b) LF Chirp, c) Boomer, d) Processed Boomer (p. 39)

Figure 6 - Comparison between a) Boomer and b) Sparker surveyed lines at the exact same place. (p. 40)

Figure 7 - HF SSS on the access channel. (p. 40)

Figure 8 - HF SSS showing the crystalline basement outcrop. (p. 41)

Figure 9 - Penetration through varied strata regarding each acoustic source. (p. 44)

Figure 10 - SSS backscatter pattern compartmentation. (p. 48)

CHAPTER 4

Figure 1 - The nautical bottom concept. Modified from Nederlof, L. (1978). (p. 55)

Figure 2 - Location of the Port of *Tubarão*. The evolution basin and the access channel are shown. The surveyed lines are identified in blue boxes and the sediments sampling sites are identified in red. (p. 57)

Figure 3 - Densitometric profiles (depth versus density) and sediment content (pizza charts) for the twelve surveyed sites (Y axis - m, X axis - kg/m^3). (p. 59/60)

Figure 4 - Chirp data from Transect T4 (evolution basin showing). a) LF (2-10 kHz) profile, b) HF (10-20 kHz) profile. The mud layer is observed while in the middle of the basin no mud is seen. (p. 60)

Figure 5 - a) and b) echograms from transect T3 (evolution basin), c) and d) echograms from transect T10 (navigation channel). Low reflection zones are seen above the yellow lines, and high reflection zones are seen above green lines. (p. 62)

Figure 6 - Single-beam dual frequency echosounder data for transect T4 showing "detachment" (in yellow) from the 38 kHz frequency in orange and the 200 kHz frequency in blue. (p. 63)

Figure 7 - Mud thickness map from the seismic profiles. (p. 64)

Figure 8 - Mud thickness map from the single beam echosounder profiles. (p. 65)

Figure 9 - Bingham yield stress versus density for the two tested calibration samples. The exponential trend adjustments are shown. (p. 66)

TABLE OF CONTENTS

| | |
|---|-----------|
| CHAPTER 1 – INTRODUCTION | 11 |
| 1. STUDY AREA | 13 |
| 2. OUTLINES AND STRUCTURE | 14 |
| 3. REFERENCES | 15 |
| CHAPTER 2 – SCIENTIFIC BACKGROUND | 18 |
| 1. ACOUSTIC WAVES | 18 |
| 2. ACOUSTIC SOURCES | 29 |
| <i>I. SEISMIC SOURCES</i> | 22 |
| <i>II. SIDE SCAN SONAR</i> | 23 |
| <i>III. BATHYMETRY AND BACKSCATTER</i> | 25 |
| 3. DENSITOMETRY | 26 |
| 4. REFERENCES | 27 |
| CHAPTER 3 – MULTIFREQUENCY GEOACOUSTIC APPROACH IN PORT'S NAVIGABLE WATERS | 29 |
| 1. INTRODUCTION | 29 |
| 2. METHODS | 32 |
| 3. RESULTS | 34 |
| <i>3.1 SEISMIC AND SIDESCAN SONAR INTEGRATION</i> | 41 |
| 4. DISCUSSION | 42 |
| 5. CONCLUSION | 49 |
| 6. REFERENCES | 51 |
| CHAPTER 4 - GEOACOUSTIC AND DENSITOMETRIC METHODS AS A TOOL FOR ASSESSING THE NAUTICAL DEPTH | 53 |
| 1. INTRODUCTION | 53 |
| 2. METHODS | 57 |
| 3. RESULTS | 59 |
| 3. RESULTS | 62 |
| 4. CONCLUSION | 67 |
| 5. REFERENCES | 68 |
| CHAPTER 5 – FINAL CONSIDERATIONS | 72 |

CHAPTER 1

INTRODUCTION

Geoacoustic methods are a set of indirect geophysical investigation techniques that have great relevance in the study of submerged areas and stand out from direct methods since they allow easy access to the underwater sites, thus enabling continuous observation of the maritime seabed and subsurface. They are feasible methods for the observation of large and continuous areas and constitute non-destructive methods (Telford et al, 1990).

Kearey et al (2009) showed that acoustics studies of high resolution in shallow water environments have been advancing on activities such as civil building projects, fishing resources, risk to navigability and dredging activities among others. Souza (2006) reviewed the use of these methods in shallow water environments and pointed out the enormous range of investigative possibilities using a wide range of geoacoustic equipment and the whole spectrum of frequencies currently available.

Marine geophysical research can be divided according to the environment to be explored. Shallow and deep water are the two main areas of investigation. Souza (2006) identified shallow environments as those delimited to 50 meters water depth, equivalent to the isobaths that approximately delimits the internal continental shelf in Brazil. Areas included are coastal, internal continental shelf, rivers, natural or artificial lakes. Deep environments are described by areas of water column of hundreds or thousands of meters, like some outer continental shelves, continental slope and ocean basins. Such compartmentation directly influences on the instrumentation and technology required to explore each type of environment.

Shallow water environment comprises coastal areas with depths of a few tens of meters, such as ports wherefore lighter equipment and lighter power sources are required, generally less than 300 to 500 J. For deep-water survey environments, with water depths of hundreds up to thousands of meters, larger vessels and more powerful and robust energy sources are needed, generally used for the petroleum industry in the deep ocean reservoirs.

Ports and navigable waterways are included in the shallow water category since they generally have shallow depths and research targets that correspond to a few tens of meters below the water column. In these environments the acoustic methods are massively used to determine the navigation risks due to silting or geohazards on the navigation channel and evolution basin, volume computation for maintenance and deepening dredging.

The maintenance of navigable waterways has always been a concern for ports management, local maritime authority and government. Ports generate huge demands for resources and efforts in monitoring and maintenance. The more silting dynamics and seabed and subsurface knowledge is undertaken the better will be the costs management and the understanding for dredging activities and possible ports expansion projects.

Dredging is the process of landfilling, excavation, removal of soil, sediments or rocks from the bottom of rivers, lakes and other bodies of water (Bray and Cohen, 2010). Dredging can be characterized in the following types: implantation, landfill, maintenance and mining. For port regions, the main activities are: dredging of implantation (operation for implantation of navigation channels and evolution basins), extension or deepening of existing access channels and maintenance (Bray, 2008).

The need for maintenance dredging comes from the constant silting process due to hydrodynamic conditions commonly seen in port regions. Continuous mud deposition may be a threat to navigation and might cause considerable reductions in nautical depth as seen by Wolanski et al., (1992), Quaresma et al., (2011) and Bastos et al., (2009). The dredging process can be very problematic for the benthic community and spread concentrated pollutants, as dredging causes resuspension of highly contaminated sediments (McAnally et al, 2007). The Brazilian Navy in its Manual of Operational Restrictions, determines that only layers with densities under 1200 kg/m^3 are safe for navigation and in other cases maintenance dredging is needed.

One of the initial stages of the consolidation process and formation of cohesive bottoms is the fluid mud (McNally, 2007). This highly concentrated suspension is associated with the sedimentation process in areas with large supply of fine sediments and periods of lower turbulence (Ross & Mehta, 1989). This fairly fluidized suspension, presents concentration between 10 and 100 g/L and densities lower than 1200 kg/m^3 (Winterwerp & van Kestern 2004).

The identification of fluid mud is commonly performed by geoacoustic methods, (PIANC, 1997) such as the single or multibeam bathymetric echo sounder operating at high frequencies. However, when navigating in fluid mud those acoustic sources identify depths that do not necessarily represent the nautical depth, and part of the fluid mud is considered as the seabed (Mehta, 2013).

Navigation in fluid mud has not yet been well documented in Brazil, although this feature is seen in many ports in the country, such as in Rio Grande (RS), Ilha Grande (SP), Rio Potengi (RN) and at the Amazon River delta (AM). Nonetheless, nor the maritime authority (Brazilian Navy) neither the Ports authority (Coastal and Ports Directory) have yet set normative understanding for navigation through fluid mud (Noernberg & Soares, 2007). Many European ports have adopted navigation on fluid mud (i.e.: Rotterdam and Zeebrugge) and have been developing research since 1980 (Wurps, 2005; Mehta, 1987).

Mapping the seabed in areas of high sediment accumulation and muddy seabed generates a scientific discussion about the applicability of different acoustic sources and

frequencies. Some questions may arise from this understanding, such as: what are the frequencies of acoustic methods best suited to map the bottom morphology and sub-bottom strata in port areas and how reliable are those data.

1. STUDY AREA

The Port of *Tubarão* (Figure 1) owned and managed by Vale S/A, is located in Espírito Santo Bay (ESB), *Vitória/ES*. The *Ponta de Tubarão*, where the port is located, is inserted in a sector of physiographic division defined by Martin L. et. al., (1996), where there is moderate exposure to incident waves eroding the coastal tertiary deposits and forming marine abrasion terraces on the beach and lateritic concretions in the submerged zone.

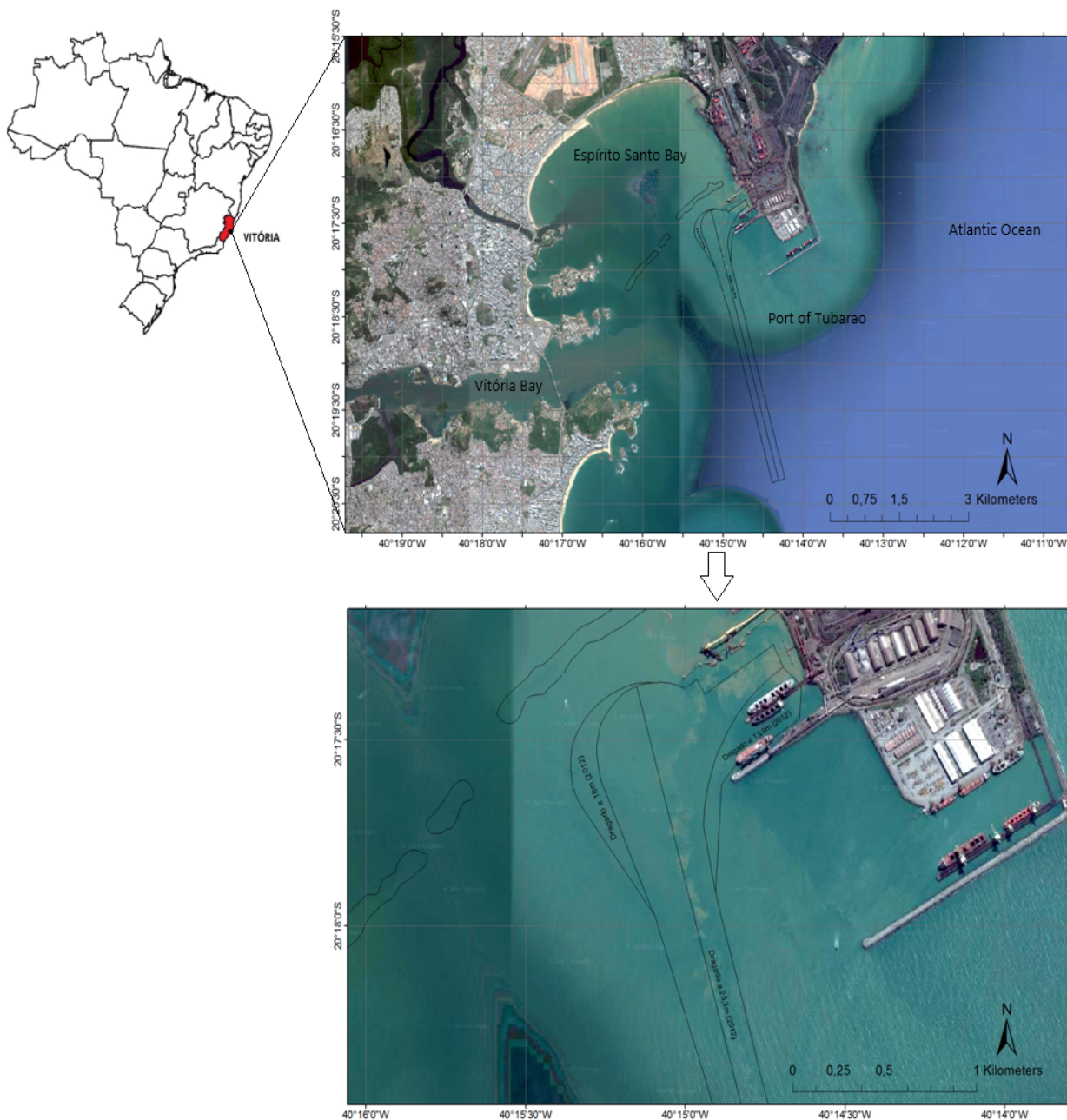


Figure 1 - Satellite image of the Port of *Tubarão*. The navigation channel and evolution basin are expressed by the continuous black line.

The ESB, previously mapped by Martin et al. (1996), Albino et al. (2006) and Carmo, (2009), Bastos et al. (2014), shows a moderate to low slope coastward. There is a region of features proud off the seabed arranged transversely in the middle of the bay. Such features can be identified as beach sandstones. Also outcrops of the crystalline gneiss basement are locally spotted near the port area.

Seismic studies performed by Loureiro et al. (2013) showed three characteristic seabed patterns in the *Tubarão* Port, being the unconsolidated surface sediments (identified as sand or mud), medium compacted clay (known as *Tabatinga*), and a more rigid material, identified as sandstone.

In studies carried out by Carmo (2009) and Bastos et al. (2014) the surface distribution of the bottom sediments of the ESB was identified, five classes were found in which the coarse to fine sand was predominant along the bay whilst mud was observed mainly in the region of the access channel and evolution basin of the port of *Tubarão*.

In the proximity of the port, litholastic sediment with low carbonate content and very fine sediments is observed. It is also observed a considerable amount of metallic minerals, probably originated from the logistic flow of products loaded into the vessels moored at the port as seen by Albino (2006), Neves et al. (2012).

The *Tubarão* Port is located on the north side of the ESB, at the Ponta de *Tubarão* (Latitude 20 ° 17'35 "South, Longitude 040 ° 14'51" West). In the table below it is possible to see details of the main areas of the port.

| Navigation Channel | | | Evolution Bay | |
|--------------------|-----------|-----------|---------------|-----------|
| Length (m) | Width (m) | Depth (m) | Radius (m) | Depth (m) |
| 4.422 | 285 | 25,3 | 365 | 13,20 |

Table 1 - Dimensions of the Port of *Tubarão*.

2. OUTLINES AND STRUCTURE

Research carried out in recent years have shown that the use of multifrequency sources offers satisfactory results in penetration and resolution in shallow water environments such as ports (Ayres Neto, 2000, Carneiro et al. 2017, Quaresma et al., 2011, Souza, 2014, Tóth et al., 1997). Therefore, for this research, it was sought to use several acoustic transducers with different frequencies to analyze how the response of these signals changes according to the characteristics of the surface and subsurface features.

This work aims to analyze and compare the conditions of reflection and resolution (for sonographic and bathymetric data) along with penetration of seismic profiling according to lithological types and integrate and analyze a wide range of data.

Multifrequency seismic data was used in the Port of *Tubarão* (*Vitória*, Brazil), in order to discuss the application of this methodology in designing engineering projects in harbors. The understanding of the acoustic response on muddy areas was assessed together with its relation to actual density values within the fluid mud layer. This assessment was made through a combination of acoustic, and *in-situ* density

measurements as well as laboratory tests. Thus, it was possible to contribute to the understanding and improvement of research in port environments, assisting in issues such as navigability, nautical depth and dredging activities agenda.

Geophysical acquisition was carried out with different equipment and different acoustic frequencies in the navigable portions of the Port of *Tubarão*. The study and characterization of these results culminated in the elaboration of this dissertation. This research is part of the call *FAPES/VALE/FAPERJ N° 01/2015 – Pelotização, Meio Ambiente e Logística* under Title of “*Dinâmica sedimentar em sistemas portuários: uma abordagem sistêmica e multidisciplinar SEDPORTOS*”.

This document is structured in five chapters, as described below.

- Chapter 1 – This section introduces the aim of the research as well as important concepts about the area of study and the structure of the dissertation.
- Chapter 2 - This section aims to present the scientific background in terms of geophysical concepts of each technique and equipment used throughout this work.
- Chapter 3 – This chapter aims to analyze the response of the acoustic signal from the multifrequency seismic approach and the dual frequency side-scan sonar in the light of penetration and resolution criteria.
- Chapter 4 – This chapter presents the same structure as the previous. The goal is to describe the correlation between acoustic data of the single-beam echosounder bathymetry with density profiles obtained through densitometric probe. The nautical depth is analyzed in the light of these methods.
- Chapter 5 – At last this chapter seeks to contextualize all the results and considerations obtained in order to summarize the use of diverse multifrequency geoacoustic methods in port areas as well as to suggest future research.

3. REFERENCES

- Albino, J.; Girardi, G.; Nascimento, K. A. 2006. *Erosão e Progradação do litoral do Espírito Santo*. In: Muehe, D. (Org.). *Erosão e Progradação do Litoral do Brasil*. Brasília: Ministério de Meio Ambiente, v. 1:226-264.
- Ayres Neto, A. 2000. Uso Da Sísmica de Reflexão de Alta Resolução e da Sonografia na Exploração Mineral Submarina. *Revista Brasileira de Geofísica*. 18(3):241-256
- Bastos A.C.; Loureiro, D.V.; Paixão, S.P. 2009. *Utilização de Métodos Geofísicos para mapeamento de Lama Fluida no Porto de Tubarão, Vitória (ES-Brasil)*. In: Anais 11º Congresso Internacional de Geofísica, Salvador (BA), Brasil.
- Bastos, A. C.; Costa Moscon, D. M.; Carmo, D.; Baptista Neto, J. A.; Quaresma, V.S. 2014. Modern sedimentation processes in a wave-dominated coastal embayment: Espírito Santo Bay, southeast Brazil. *Geo-Marine Letters* , v. 35, p. 23-36.
- Bray, R. N. 2008. *Environmental Aspects of Dredging*. Leiden (Holanda): Taylor & Francis Group.
- Bray, R. N., & Cohen, M. 2010. *Dredging for development (6th ed.)*. Haia (Holanda): International Association of Dredging Companies - IADC, International Association of Ports and Harbors – IAPH)
- Carmo, D.A. 2009. *Mapeamento Faciológico do Fundo Marinho como Ferramenta ao Entendimento da Dinâmica Sedimentar da Baía do Espírito Santo, Vitória-ES. Dissertação de Mestrado. Programa de pós graduação em geologia e geofísica marinha, UFF, Niterói, RJ, 134p.*
- Carneiro, J.C.; Fonseca, D.L.; Vinzón, S.B.; Gallo, M.N. 2017. Strategies for Measuring Fluid Mud Layers and Their Rheological Properties in Ports. *Journal of Waterway, Port, Coastal and Ocean Engineering*. v. 143 p. 04017008.
- Keary, P.; Brooks, M.; Hill, I. 2002. *An Introduction to Geophysical Exploration*, 3rd ed. Blackwell Publications, Oxford. 262 pp.
- Loureiro, D.V.; Quaresma, V.S.; Bastos, A. C. 2013. *Estudo de Caso da Dragagem do Porto de Tubarão (Vitória-ES): Utilização Integrada de Dados Geofísicos e Geotécnicos*. *Revista Brasileira de Geofísica*. n. 91, p. 24-25.
- Martin, L.; Suguio, K.; Flexor, J.M.; Archanjo, J.D. 1996. Coastal Quaternary formations of the southern part of the state of Espírito Santo (Brazil). *Academia Brasileira de Ciências*. v.68, p.389-404.
- McAnally, W.H.; ASCE. F; Friedrichs, C; Hamilton, D.; Hayter, E.; Shrestha, P.; Rodriguez, H.; Sheremet, A.; Teeter, A. 2007. Management of fluid mud in estuaries, bays and lakes. I: Present state of understanding on character and behavior. *Journal of Hydraulic Engineering*. v.133, n.1
- Mehta, A.J.; Hayter, E.J.; Parker, W.R.; Tester, A.M. 1987. Cohesive sediment transport processes. in: *Sedimentation control to reduce maintenance dredging of navigation facilities in estuaries*. Report and symposium proceeding. National Academic Press, Washington, D.C., 1987. p.53-76.
- Mehta, A.J. 2013. *An introduction to hydraulics of the fine sediment transport (Advanced series on ocean engineering) v.38 world scientific*

- Neves, R.; Quaresma, V. S.; Bastos, A. C. ; Ruano, J. 2012. *Transporte sedimentar em baías costeiras: estudo de caso nas Baías de Vitória e Espírito Santo-ES-Brasil*. *Revista Brasileira de Geofísica (Impresso)* , v. 30, p. 181-189, 2012.
- Noernberg, M. & Soares R.C.,. (2007). *A presença de lama fluida navegabilidade no canal de acesso à região portuária de Antonina (PR)*. 49º *Geology Brazilian Congress*. August 2018 – Rio de Janeiro.
- PIANC. 1997. Approach Channels: A guide for design. Report of working group No. 30 of the permanent technical committee II, supplement to bulletin No. 9. Brussels: General secretariat of the permanent international association of navigation congresses.
- Quaresma, V.S.; Bastos, A.C.; Loureiro, D.V.; Paixão, S. 2011. *Utilização de métodos geofísicos para mapeamento de lama fluida no porto de tubarão, Vitória (ES-Brasil)*. *Revista Brasileira de Geofísica*. 29(3): 487-496.
- Ross M.A; Mehta, A.J. 1989. On the mechanics of lutoclines and fluid mud. *Journal of Coastal Research*, SI5:51-62
- Souza, L.A.P. 2006. *Revisão Crítica da aplicabilidade dos métodos geofísicos na investigação de áreas submersas rasas*. Tese de Doutorado, Programa de Pós Graduação em Oceanografia Química e Geológica, IO, USP, SP. 311p.
- Souza, L.A.P. 2014. *Sísmica Multifrequencial: A Melhor Solução Para a Investigação de Ambientes Submersos Rasos*. *Laboratório Nacional De Energia E Geologia*, I.P. IX CNG/2º CoGePLiP, Porto 2014. v. 101, Especial II, p.701-705
- Tóth, T.; R. Vida; Hórvath, F. 1997. Shallow-water single and multichannel seismic profiling in a riverine environment. *Lead. Edge*, nov. 1997, p.1691-1695.
- Telford, W.M.; L.P. Geldard; R.E. Sherif; D.A. Keys. 1990. *Applied geophysics*. First Edition. Cambridge. University Press. 860p.
- Winterwerp, J; Kesteren, W.G.M. 2004 Introduction to the physics of cohesive sediment in the marine environment. *Developments in sedimentology* 56. T. van Loon, ed. Amsterdam. Elsevier. 466p.
- Wolanski, E.; Gibbs, R.J.; Maza, Y; Mehta, A. and King, B. 1992. The role of turbulence in the settling of mud flocks. *J. Coastal Research*. 8(1), 35-46.

CHAPTER 2

SCIENTIFIC BACKGROUND

Physical properties of the geological materials (unconsolidated rocks or sediments) define the behavior of waves in the investigated area and can be used for the understanding and construction of the subsurface geological history, such as density of rocks and sediments as well as properties of their elastic modulus. Each material has specific values related to their physical structure. These elastic *moduli* represent the deformation suffered by a material as a function of a force exerted on them, such as the passage of acoustic waves, as seen by Ayres Neto (2000), Jones (1999) and McGee (1995).

1. ACOUSTIC WAVES

Considering how an acoustic wave propagates through a certain material, it can be divided into (Kearey et al, 2002):

- Body waves (Figure 1): According to Schon (1996), they propagate even at high depth on solid or liquid objects. They may be compressional (longitudinal, primary or P waves, which propagate in solid and fluid media) or shear waves (transverse, secondary or S waves, which do not propagate on fluids);

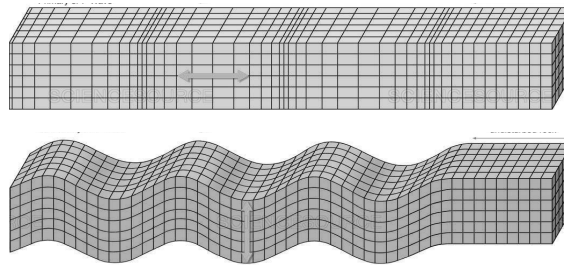


Figure 1 - Elastic deformation and particle motion.
a) Primary and b) Secondary Wave, Telford et al. (1990).

The velocity of propagation of the P and S waves can be defined according to the relationship (Equation 1) between the density of the media and the elastic *moduli* (Schon 1996):

$$\text{(Equation 1)} \quad V_p = \sqrt{\frac{k + \frac{4}{3}\mu}{\rho}} \quad V_s = \sqrt{\frac{\mu}{\rho}}$$

Where V_p is the velocity of the primary wave, V_s is the velocity of the secondary wave, k is the incompressibility module, μ is the rigidity and ρ is the density of the material.

- Surface waves (Figure 2): The author *op. cit* also shows that these waves are confined to the outer portion of the solid earth (Love or Rayleigh) types. They are not relevant for the marine geophysics due to their ineffective propagation in fluids.

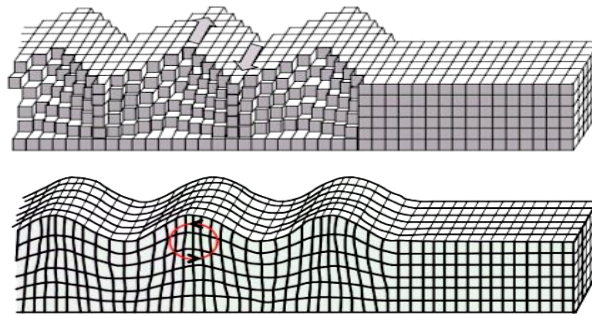


Figure 2 - Elastic deformation and particle motion.
a) Rayleigh and b) Love waves. Telford et al. (1990).

Acoustic body waves are poorly absorbed by water, allowing surveys in shallow and deep-water regions (Kearey et al., 2002). The effects of propagation, reflection and refraction of acoustic waves on the surface and marine subsurface allow inferring the morphological and sedimentological characteristics of the geological materials investigated. It is known that rocks and sedimentary structures that vary in density and composition according to depth and distribution form the seabed (Schon, 1996).

The reflection and refraction phenomena are described by Snell's Law (Figure 3), which relates two distinct media and their properties to the angle of incidence of the wave in their contacts. The P wave suffers a split into two components as it interacts at the boundary between distinct physical property interfaces. There is a separation on a reflected wave, with velocity V_1 at the same angle θ_1 of the incident wave and a refracted wave, as seen in Equation 2 (Cervency, 1971).

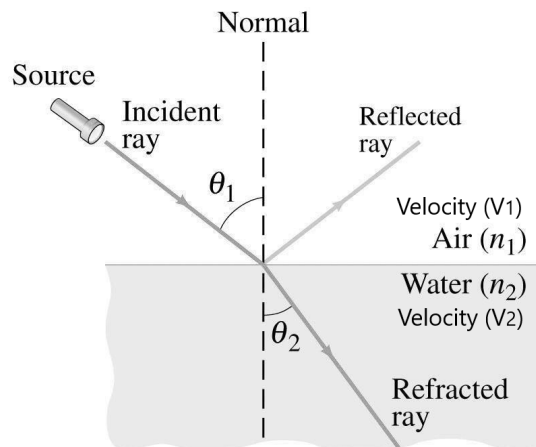


Figure 3 - Snell's Law for reflection and refraction, Telford (1990).

(Equation 2)

$$\frac{\sin\theta_1}{\sin\theta_2} = \frac{V_1}{V_2}$$

Jackson et al. (2007), Cervency (1971), Schon (1996), Ayres Neto & Theilen (1999) shows that in the event of the emission and propagation of the acoustic pulses, the transmission of the acoustic wave through the water column occurs, without great losses or attenuation due to physical characteristics of the seawater. Once these pulses reach the object of interest and pass through it and propagate in the deeper layers, part of that energy is reflected back to the acoustic receivers, which are responsible for reading the acoustic signal return, and are then converted into electrical impulses, interpreted as physical characteristics of the geological materials.

Acoustic waves are produced and released by the transducers or acoustic sources of the geophysical equipment in which occurs the generation of a wave commonly produced by piezoelectric materials McGee (1995).

The elastic characteristics of the medium will define how the wave will behave. The produced waves have specific geometry and intensity, according to the configuration of the equipment that generated them. The wavelength refers to the distance between the crests of the waves, measured at the same point in each wave. Wave frequency is the number of waves that pass in a second at a specific point. The measurement cycles are called Hertz (McGee, 1995).

The frequency of the elastic wave (Figure 4) produced by the transducers is inversely proportional to the energy required to produce such wave and how much will translate in penetration and resolution of the underwater geological substrates. Smaller frequencies produce data with lower resolution but with higher penetration. Therefore require more energy for its generation (Ayres Neto, 2000).

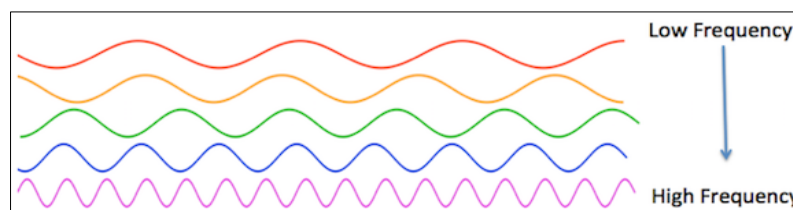


Figure 4 - Relation between waveform and frequency.

Generally, sediments found in the surficial layers of the seafloor are not consolidated. The consolidation degree varies according to depth, material type, hydrodynamic conditions and geological factors. Physical properties such as porosity and density are used in the interpretation of the geoacoustic data once the physical characteristics are known through literature. The properties of the acoustic waves are influenced by physical factors of the sediments and how they are arranged: porosity, granulometry, compressibility, organic matter/gas content and permeability (Telford, 1990).

The reflection and refraction of the wave will influence the amount of energy reflected and transmitted at an interface between two distinct geological boundaries, characterizing the seismic reflectors (i.e. seismic) or in the signal intensity and backscattering (i.e. side scan sonar) (Blondel, 2009).

2. ACOUSTIC SOURCES

The theory described below regarding the acoustic sources functioning is mainly based on the fourth chapter of the Applied Geophysics Book by Telford et al. (1990). The operation of acoustic geophysical acquisition equipment follows a pattern: the signal or wave is produced at the source or transducer through the transformation of an electric pulse into mechanical energy, that pulse travels through the water column, reaches the targeted geological object (whether in surface or subsurface), it undergoes physical effects of reflection, refraction, attenuation, scattering then the signal finally returns to the acoustic receiver where it is converted into electric pulses and then manipulated into interpretable properties by the acquisition software. The way the acoustic waves are produced can be used to categorize different types of sources:

- Resonant sources have the advantage of operational ease because of their good maneuverability due to their small size, low maintenance cost, high repeatability and efficiency (high signal-to-noise ratio). These sources include the ones used for conventional bathymetry (echosounders), side scan sonar, and seismic sources such as Chirps and parametric transducers. The disadvantage lies in the relative low penetration compared to other acoustic sources, up to a few tens of meters, depending on the subsurface content (McGee 1995 and Mosher & Simpkin 1999).
- Impulsive sources release a large amount of energy in an interval of time ideally close to zero and are capable of producing waves with high amplitude and length, leading to low frequencies. These sources show higher penetration although there is a loss in vertical resolution. The way the acoustic waves are produced is used as a parameter to characterize some impulsive sources, such as by mass acceleration (boomer), implosive (watergun) and explosive sources (i.e.: sparkers) (McGee 1995).

Souza (2013) suggests a classification of geoacoustic sources according to the research goal, divided into two main groups: bottom and sub-bottom research (Figure 5).

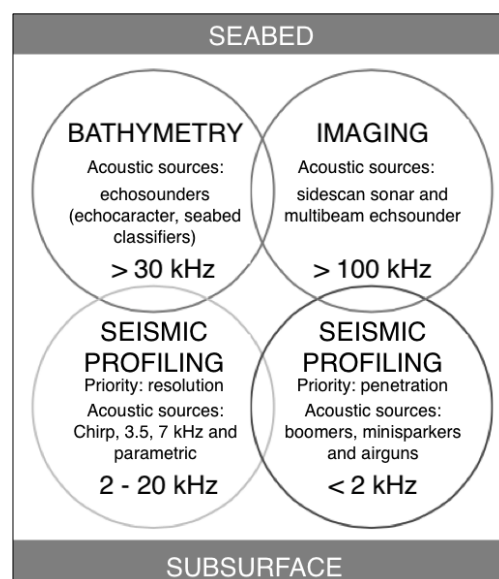


Figure 5 - Environment investigation and suggested sources.
Modified from Souza (2013).

I. SEISMIC SOURCES

Seismic profiling is a geophysical for subsurface investigation. Mosher et al. (1999), and Missimer et al. (1976) show that the penetration and vertical/horizontal resolution are features dependent on the frequency of the signal generated in the acoustic source or transducer. Its physical principle determines the time that a wave leaves the source by propagation velocity, reaches the seismic reflectors and returns to the receiver (hydrophone or transducer), thus estimating the depth and acoustic impedance of the geological contacts. The seismic profile obtained can help infer details about stratigraphy in the most diverse scales.

The acoustic impedance (I_1) is given as the product of the velocity of sound propagation (V_1) in a medium by the density (δ_1) of that medium (Equation 3).

(Equation 3)
$$I_1 = V_1 * \delta_1$$

The relation of the angles of normal incidence to the reflecting surface is the reflection coefficient (R) and can be obtained as the ratio between the amplitude of the reflected signal and the amplitude of the incident wave, represented by the Equation 4.

(Equation 4)
$$R = \frac{I_2 - I_1}{I_2 + I_1} = \frac{\delta_2 V_2 - \delta_1 V_1}{\delta_2 V_2 + \delta_1 V_1}$$

The reflection coefficient depends on the acoustic impedance contrast between the two physical media, such interfaces are characterized in the seismic records as reflecting horizons or simply seismic reflectors, thus delimiting possible geological layers (Ayres Neto, 2000).

In shallow water seismic reflection, sources such as boomers, sparkers and chirps are used to investigate subsurface areas, these equipment emit a wide frequency range, allowing resolution of up to centimeters and the penetration can reach up to a couple of hundreds of meters, depending on the material they propagate through (Figure 6) (Souza, 2013).

a) Boomer-type sources are commonly used in the investigation for shallow water environments. They are electromagnetically driven sound sources usually mounted on a towed catamaran. The navigation positioning is not as precise as with systems where the source and receiver(s) are directly adjacent (pole or hull mounted). It is possible to reach up to 200 meters of penetration in saturated sandy sediments (Simpkin, 2005).

b) The Sparker is an explosive-type source. Its operation is based on an electric discharge generated by an electrode dipped in a conducting medium (sea water). The rapid and explosive emission of the electric discharge in the sea water creates vapor bubbles, when rapidly expanded generate a positive impulse that propagates in the water column generating seismic pulses.

c) Chirp-type sources can be separated into low-resolution (2-8 kHz), high-resolution (10-20 kHz), and even very-high-resolution (20-50 kHz), they allow considerable energy and frequency emission control and consequent directivity and great resolution/penetration ratio. Because of the very high frequencies produced, they have great vertical resolution but reach penetration of only a couple of tens of meters, for the lower frequencies and only a few meters for the higher frequencies, depending on the strata (Souza 2006).

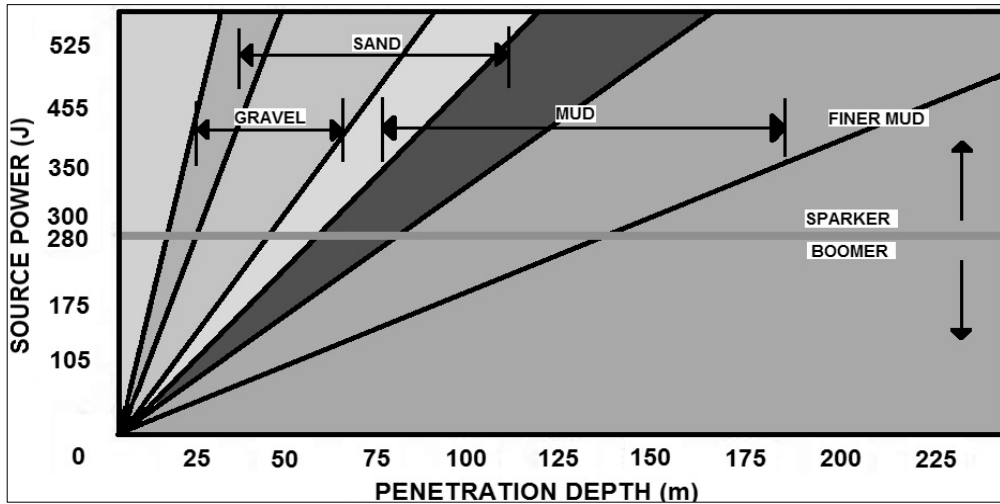


Figure 6 - Comparison of the expected penetration between the sources Boomer (GeoPulse Applied Acoustics model) and Sparker. Modified from <<http://www.geoacoustics.com>> November/2018

II. SIDE SCAN SONAR

The Sidescan sonar (SSS) emits high frequency acoustic signals (50 to 1600 kHz) at regular time intervals through two transducers (emitter and receiver) located on both sides of the object (port and starboard), known as fish, towed by the vessel.

The SSS's transducers are made up of sets of piezoelectric parts that convert electrical voltage to mechanical energy and propagate that energy through the water column (Souza 2006). The data obtained are generated through the return of signals (backscatter) that reach the seabed and return to the receiver with characteristics corresponding to a series of factors (Morang et al., 1997) such as the type and texture of the surface sediment, angle of incidence of the signal, micromorphology of the seafloor, attenuation of sound waves and degree of sediment compaction (Blondel & Murton, 1997). The definition and recognition of reflection patterns are based on signal intensity and texture patterns (Ayres Neto & Aguiar, 1993).

The SSS obtains mosaics of the seabed, similar to two-dimensional images (Figure 7). The acquired imagery is useful in many engineering and oceanographic fields such as nautical chart construction, underwater object identification, geological risk studies, geotechnics and oceanography of submerged environments and even in search and rescue operations, i.e.: Preston et al. (2004), Quaresma et al. (2000), Collier & Brown (2005) and Souza (2006).

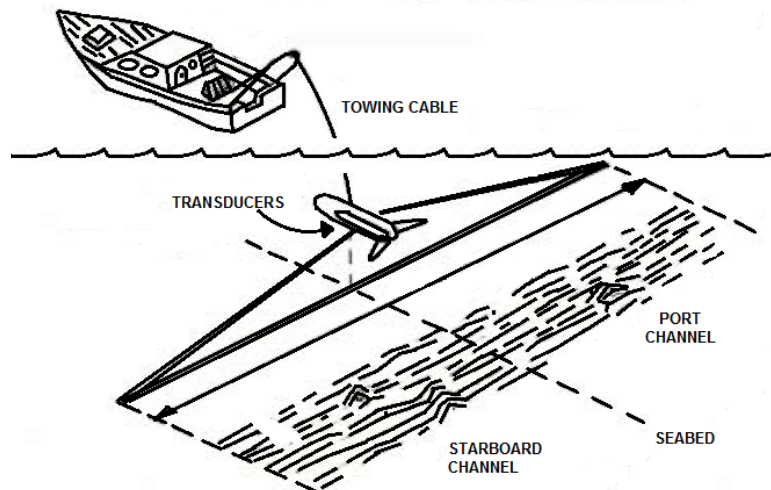


Figure 7 - Side Scan sonar acquisition geometry. Modified from Mazel (1985).

High frequency acoustic signals are highly attenuated by seawater and low frequency signals are reduced at a much lower rate. Therefore, 50Hz acoustic pulses can be transmitted for thousands of miles while 100 kHz pulses can only be transmitted up to a maximum of 1 or 2 km. It is estimated that the fish should be towed at a height equivalent to 10% of the lateral swath range reached. Thus, on a survey where lateral reach of 100 meters is sought, the fish should be kept at a height of 10 meters from the bottom surface (Kearey et al. 2002 and Souza, 2006).

Other features are related to resolution such as the signal beam width and pulse duration. In the interaction of the SSS signal with the seabed, two phenomena occur: reflection and backscattering (Figure 8).

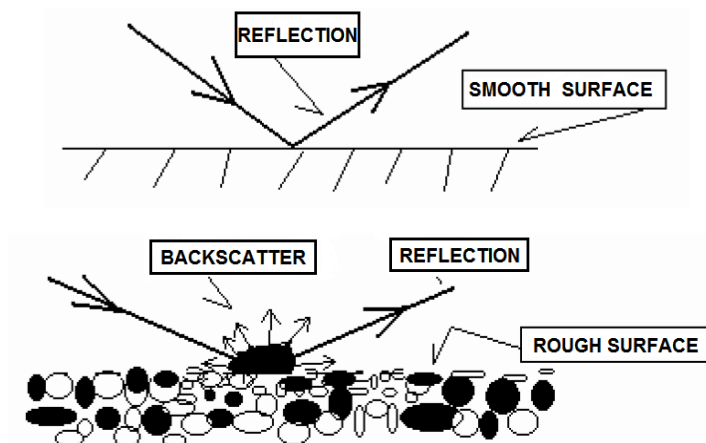


Figure 8 - Reflection and backscattering by the SSS. Modified from Mazel (1985).

Reflection occurs when the signal reaches the bottom surface and randomly returns at different angles, some of the waves return to the transducer. Backscatter relies on the interaction between the acoustic waves signal energy and the texture of the seabed material and the consequent intensity of the return signal. Backscatter is closely linked to the irregularities seen on the seabed, causing the emitted signal to undergo a spreading event. Therefore, the rougher the surface, the lower the incidence angle and the greater the signal return intensity to the transducer (Flemming, B.W. 1976).

III. BATHYMETRY AND BACKSCATTER

Bathymetry determines the thickness of the water column calculated based on the two-way travel time of the reflection of the acoustic waves on the seabed. A transducer, known as echosounder, which can be hull or pole mounted on the vessel, emits acoustic waves. Depth calculation is performed by the time travel and speed of the acoustic signal from and to the receiver (Clay & Medwin, 1977). Acoustic signals that return faster to receivers refer to shallower areas, while deeper areas result in a longer time to return. Acoustic wave speeds may also vary depending on temperature, salinity and pressure (Telford et al 1990).

Echosounders transducers are made of a piezoelectric ceramic material that undergoes millimetric changes of size in the event of electric current applied thereto producing sound waves, thus transmitting a pressure wave with a specific frequency into the water. Upon the return of this pulse after its reflection, the pulse is converted into electrical signals by the transducer and converted into depth data (Hughes Clarke, J 2000).

For single-beam echosounders (SBES), acoustic pulses emitted by the source spread out in the form of a narrow cone and return in the same manner to the receiver (Figure 9). Wave cones with wider angles display large areas of the bottom surface and negatively affect system resolution. The opposite occurs when using systems with narrow signal bundles (Clay & Medwin, 1977).

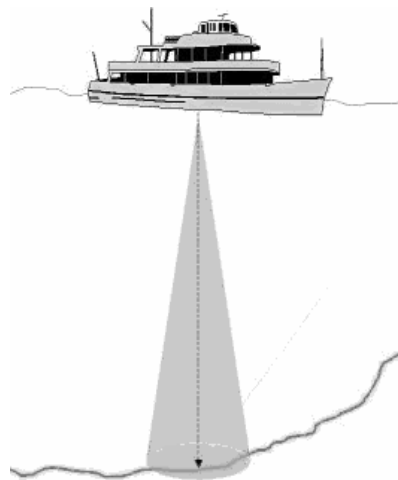


Figure 9 - Singlebeam echo sounder operation.

Echosounders work with high frequency signals, generally higher than 8, 15, 24 and 30kHz. Currently, dual-frequency SBES working simultaneously with 24, 33 or 38 and 200kHz are used for both deep and shallow water. Depending on the substrate nature, low-frequency echosounders (below 50kHz) also allow the acoustic signal to penetrate through superficial layers of sediments (Souza, 2014).

Conventional single-beam bathymetry systems measure the depth of the water column immediately below the vessel vertically along the research profile, which means that to obtain a precise bathymetric map, a large number of bathymetric profiles parallel to each other is required although it is still possible for interlinear features between these

profiles to go unnoticed. The solution for this problem came with the creation of equipment able to emit sound waves in a fan shape, also known as multibeam echosounder (Hughes-Clarke et al., 1996 and Blondel & Murton, 1997).

3. DENSITOMETRY

Densitometry is a technique for measuring the density of fluid materials. It is widely used when there are materials formed by more than one type of substance. In the geological context, this tool is useful for muddy seabed. Data acquisition with this tool can be used for assessment of navigation in fluid mud and to improve dredging activities by determining densities and depth *in-situ*, (Figure 11) (Fontein & Byrd, 2007).

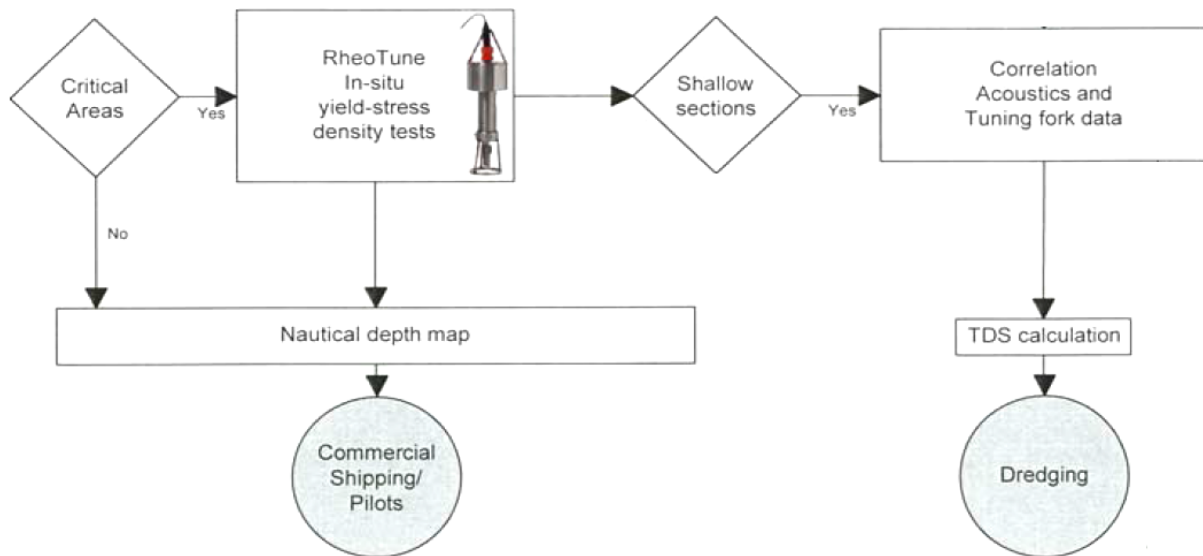


Figure 10 - Combined nautical depth survey scheme. Modified from Fontein & Byrd (2007).

The probe works based on the principle that the density of the media in which it is immersed in is responsible for the resonant frequency of the piezometric element at its acoustic source. For different rheology parameters, a frequency/density and viscosity ratio is obtained (Fontein & Byrd, 2007).

According to the author *op cit.*, the acoustic density measurement system is based on the seismic reflection theory. The reflected energy is governed by impedance contrasts. The high-water content in the mud mostly governs the velocity of sound in that medium and shows little change in the fluid material. After a compensation calibration, the system can calculate the density starting from the return of the acoustic signal.

The tuning fork has a resonant frequency close to 1kHz in vacuum at a given frequency by applying a voltage to a piezoelectric element located at its base. The natural resonant frequency of the vibrating fork sensor decreases as the density of the fluid mud increases, and the amplitude of vibrations decreases with increasing viscosity (Zheng et al., 2012). The densitometry apparatus descends from the vessel to the seafloor in order to produce a density profile as it advances through the water column, traversing the seabed layer of sediment from the bottom.

4. REFERENCES

- Ayres Neto, A.; Aguiar, A.C.K.V. 1993. *Interpretação de reflexões de sidescan: uma proposta de nomenclatura e padronização de métodos. In: Congresso Internacional da Sociedade Brasileira de Geofísica, 3. Rio de Janeiro, RJ. Boletim de resumos expandidos.*
- Ayres Neto, A. 2000. Uso Da Sísmica de Reflexão de Alta Resolução e da Sonografia na Exploração Mineral Submarina. *Revista Brasileira de Geofísica.* 18(3):241-256
- Ayres Neto, A.; Theilen, F. 1999. Relationship between P- and S-wave velocities and geological properties of near-surface sediments of the continental slope of the Barents Sea. *Geophysical prospecting,* 47:431-441.
- Ayres Neto, A. 2000. *Uso Da Sísmica de Reflexão de Alta Resolução e da Sonografia na Exploração Mineral Submarina. Revista Brasileira de Geofísica.* 18(3):241-256
- Blondel, P. & Murton, B. (1997). *Handbook of Seafloor Sonar Imagery.* Wiley Praxis Series in Remote Sensing.
- Blondel, F., 2009. *The Handbook of Side Scan Sonar.* Praxis Publishing Ltd, Chichester UK. 344pp.
- Cervency, V.; Ravindra, R. 1971. *Theory of Seismic Head Waves.* Toronto: Toronto University Press.
- Clay, C.S.; Medwin, H. *Acoustical Oceanography: Principles and Applications,* John Wiley and Sons, New York (1977). *Journal of Sound and Vibration,* Volume 60, Issue 4, p. 615-616.
- Collier, J.S. & C.J. Brown. 2005. Correlation of sidescan backscatter with grain size distribution of surficial seabed sediments. *Mar. Geol.,* 214(4):431-449.
- Flemming, B.W. 1976. Side Scan Sonar: a practical guide. *Int. Hydrogr. Rev.* 53(1), 28p.
- Fontein, W.F; Byrd, R.W. 2007. The nautical depth approach, a review for implementation. *Wodcon XVIII Annual Dredging Seminar.*
- Hughes-Clarke J.E.; Mayer L.A.; Wells D.E. 1996. Shallow-water imaging multibeam sonars: a new tool for investigating seafloor processes in the coastal zone and on the continental shelf. *Marine Geophysical Research* 1996; 18:607-29.
- Hughes Clarke, J.E. 2000. Present-day methods of depth measurements: Continental shelf limits, in Cook, P.K. and Carleton, C.M., eds., *The scientific and legal interface:* Oxford University Press, p. 139-159
- Jackson, D.R.; Richardson, M.D. 2007. *High-frequency seafloor acoustics.* Springer, 616 pp.
- Jones, E.J.W. 1999. *Marine geophysics.* Baffins Lane, Chichester, John Willey & Sons Ltd. Inc. 466p.
- Keary, P.; Brooks, M.; Hill, I. 2002. *An Introduction to Geophysical Exploration,* 3rd ed. Blackwell Publications, Oxford. 262 pp.
- Mazel, C. 1985. *Side Scan Sonar training manual.* New York, Klein Associates. Inc. Undersea Search and Survey. 144p.
- McGee, T.M. 1995. High-resolution marine reflection profiling for engineering and environmental purposes Part A: Acquiring analogue seismic signals. *J. Applied Geophysics.* 33(4):271-285.

- Missimer, T.M., Gardner, R.A. 1976. High-resolution Seismic Reflection Profiling for Mapping Shallow Water Aquifers in Lee County. FL. U.S. Geological Survey, Water Resources Investigation. 45-75, 30 p.
- Morang, A.; Larson, R.; Gorman, L. 1997. Monitoring the coastal environment; Part III: Geophysical and Research Methods. *Journal of Coastal Research*, 13 (4):1064-1085
- Mosher, D.C.; Simpkin, P. 1999. Status and trends of marine high resolution seismic reflection profiling: data acquisition. *Geosci. Can.*, 26:174-188
- Preston, J.M.; A .C. Christney; W .T . Collins & S. Bloomer . 2004. Automated acoustic classification of sidescan images. In: *Oceans 2004*, 9 a 12 de novembro de 2004, Kobe, Japan.
- Quaresma, V. S.; G.T.M. Dias & J.A. Baptista Neto. 2000. Caracterização da ocorrência de padrões de sonar de varredura lateral e sísmica de alta frequência (3,5 e 7,0 kHz) na porção sul da Baía de Guanabara. *J. Rev. Bras. Geof.*, 18(2):201-214.
- Schön, J.H., 1996. Physical Properties of Rocks. Fundamentals and Principles of Petrophysics. Handbook of Geophysical Exploration. Section I, Seismic Exploration, V.18. Pergamon Press. 583 pp.
- Sharma, P.V., 1997. Environmental and Engineering Geophysics. Cambridge University Press. 475 pp.
- Simpkin, P.G. 2005. The Boomer sound source as a tool for shallow water geophysical exploration. *Mar. Geophys. Res.*, 26(2):171-181
- Souza, L.A.P. 2006. *Revisão Crítica da aplicabilidade dos métodos geofísicos na investigação de áreas submersas rasas. Tese de Doutorado, Programa de Pós Graduação em Oceanografia Química e Geológica*, IO, USP, SP. 311p.
- Souza, L. A. P & Gandolfo, O. C. B. 2013. *Métodos geofísicos em geotécnica e geologia ambiental. Revista Brasileira de Geologia de Engenharia e Ambiental*. ABGE. Vol. 2 pp. 9-27.
- Telford, W.M.; L.P. Geldard; R.E. Sherif; D.A. Keys. 1990. Applied geophysics. First Edition. Cambridge. University Press. 860p.
- Zheng, D., Shi, J., & Fan, S. (2012). Design and theoretical analysis of a resonant sensor for liquid density measurement. *Sensors (Basel, Switzerland)*, 12(6), 7905-16.

CHAPTER 3

THE MULTIFREQUENCY GEOACOUSTIC APPROACH IN PORT'S NAVIGABLE WATERS

Abstract

Acoustic methods are widely applied in ports and harbors for the determination of navigation hazards, support to dredging and rock-excavation and/or expansion projects, stimulating discussions on the applicability of various seismic techniques employing different acoustic sources emitting a spectrum of frequencies. There is a wide range of equipment or acoustic systems available, which can generate products with very high vertical resolution (high frequencies) or high penetration (low frequencies). The simultaneous use of different acoustic sources enables acquisition of seismic profiles with both resolution and penetration quality. The multifrequency acoustic approach was applied in the Port of *Tubarão* (*Vitória*, Brazil) in order to provide subsidies for designing engineering and monitoring projects in harbors. Two impulsive sources (boomer and sparker, frequencies <2 kHz), two resonant sources (chirps, frequencies between 10-20 kHz and 2-8 kHz, respectively) and a double frequency SSS (455 / 900 kHz) were employed. Such approach enabled the detailed mapping from the point of view of resolution and penetration.

Keywords: multifrequency, seismic, ports, harbors, dredging, navigability, fluid mud, shallow-water.

1. INTRODUCTION

Applied geoacoustic methods in port regions such as seismic and side-scan sonar are important components in determining navigation hazards, designing engineering construction, support to dredging, rock-excavation and expansion projects.

Acoustic methods can also be applied for silting monitoring and nautical bottom reports to the relevant regulatory body, stimulating discussions on the applicability of various acoustic sources simultaneously emitting different frequency spectra. (Jones, 1999; Souza, 2006; Atherton, 2011; Fish, Cara & Arnold, 1990; Blondel, 2009; Mosher & Simpkin, 1999).

Seismic methods are of great importance in such environments due to the range of equipment or acoustic systems available, which allow generating products with high vertical resolution (high frequencies) or high penetration (low frequencies). Sonar imaging allows an instant visualization of the surface morphological features associated with lithology. The multifrequency approach allows all these data to be obtained in the same acquisition procedure.

High frequency systems are efficient for mapping the seabed surface and side-scan sonar systems are one of the main tools in this group (Souza et al., 2007; Souza et al.,

2009; Souza, 2008). Low energy and high frequency resonant seismic systems like Chirps, operating at frequencies from 2 kHz up to 50 kHz, offer high or ultra-high vertical resolution profiles and are able to identify shallow sediment strata to within a few centimeters in thickness (Souza, 2013).

Low frequency systems are employed for subsurface mapping, being able to obtain data from shallow interfaces to deep reflectors (Souza, 2013). Boomers and sparkers are this group's most common sources. They allow the acquisition of seismic reflectors up to more than 100 m deep. Reflectors are interfaces between layers of contrasting acoustic properties and might represent a change in lithology, faults or nonconformities (Telford, 1990).

Effectively, most port designing engineering projects require products that allow an approach from the point of view of both resolution and penetration. Thus, the best solution is to deal with a wide spectrum of frequencies, in a simultaneous multi frequency approach, in order to guarantee maximization of product quality control, minimizing operational costs (Ayres Neto, 2000; Carneiro et al., 2017; Gallea et al., 1989; Loureiro, 2011; Quaresma et al., 2011; Souza, 2014; Tóth et al., 1997).

A limiting factor for ports is their ability to receive larger ships which represents an increase of their profitability. For this purpose, it is necessary that the maximum navigable depth is deep enough to maintain safe navigation for these vessels. Therefore, deepening dredging projects are necessary and the complete mapping of the surface and subsurface of the site is of extreme importance for designing the best dredging equipment, need for rock excavation, environmental impacts and many other issues regarding port areas.

The port of *Tubarão* (Vale Company), one of the most important ore exporting Ports in Brazil, located at *Ponta de Tubarão* on the north of *Espírito Santo* Bay, *Vitória*/Brazil went through a deepening dredging from the year of 2012 to 2013, increasing navigation depths from 22 m to 25 m in the evolution basin and navigation channel, in order to allow the passage of large scale vessels such as the VALEMAX, capable of transporting up to 400.000 ton.

Due to several past deepening and maintenance dredging activities, the port has reached areas with exposed sedimentary rocks and crystalline basement outcrops. Several of these features are described in studies published by Albino (2006), Carmo (2009), Bastos (2014) and Loureiro (2013), who identified sedimentary rocks, compacted clay (*Tabatinga*) and crystalline basement outcrops. Due to the hydrodynamic conditions of the area and the contribution of fine sediments from continental origin, fluid mud is present throughout the port's underwater areas.

Therefore, we assessed an approach capable of investigating both surface and subsurface features simultaneously, indicating the behavior of different frequencies in various substrates present in the studied port. Dredging projects can be performed more accurately and port monitoring can become more efficient. Aiming at the development of geoacoustic research in port environments and assisting in issues such as navigability, nautical depth and dredging projects.

2. METHODS

Resonant sources, such as the high frequency Chirp (10-20kHz), with high vertical resolution and lower penetration and a low frequency Chirp (29 kHz) with lower vertical resolution and higher penetration (Meridata Finland), were used. Impulsive-type sources were also used, such as the SIG Boomer (0.5-2kHz) and the explosive-type SIG ELC820 Sparker (0.9–1.4kHz).

Seismic data were acquired simultaneously through the multifrequency multi-mode system MD-DSS Meridata, through the MDCS software. The sonographic acquisition was made using the Klein 4900 double-frequency side-scan (455/900 kHz), operated at an average depth of 10 meters off the seabed and utilizing the acquisition software SonarPro.

Seismic data were initially processed using the software Chesapeake SonarWiz, Meridata MDPS, SeiSee and interpreted through IHS Kingdom. For the interpretation, each seismic line was analyzed together with the sonar images, aiming to identify the mud layer, the outcropping acoustic basement and the relation between penetration, resolution and subsurface strata.

Positioning was acquired by a GNSS DGPS Receiver system operating with two antennas. A geometric arrangement of the sources was settled so there was no interaction between the emitted frequencies, improving the signal-to-noise ratio. The Sparker and Boomer were alternated during the acquisition because of the following reasons: both are towed and produce similar frequency spectra, the Meridata acquisition system does not allow both sources to function together and the sparker source available for this research would wear out its electrical components. 26 transverse and 5 longitudinal lines were surveyed along the entire length of the evolution basin and the access channel of the Port of *Tubarão* (Fig. 1).

Due to the great attenuation loss and depth absorption, boomer and sparker data were processed using the Seismic Unix software in order to gain in-depth visualization with lateral continuity and allow better assessment and interpretation of the subsurface features.

Through the SonarWiz software, the seismic horizons were plotted for the mud package, for the consolidated material, corresponding to stone or compacted clay and for the top of the crystalline basement for each seismic frequency. Thickness and penetration maps were built.

Every seismic continuous seismic horizon was identified and interpreted, their depths were calculated and fed onto a spreadsheet where different seismic sources could be compared in terms of penetration in meters. Also, resolution analysis was performed by calculating vertical measurements between homologue seismic horizons in centimeters, therefore every source could also be compared in terms of resolution. Similar calculations were performed for the sidescan data, where resolution was assessed by the imagery analysis. Resolution values were fed onto a spreadsheet and low and high resolution could be compared in terms of centimeters.

For a sedimentological understanding, surficial material was collected at 16 stations using a Van-Veen grab sampler, the sites for sediment sampling were chosen during the

survey based on the response of the geoaoustic data, it was intended to collect samples were layers of mud and/or unconsolidated sediment were seen. The samples were processed in the laboratory, performing a laser particle size analysis (Mastersize 2000, Malvern Instruments) (Amos & Sutherland, 1994). Data from previous geotechnical and geophysical surveys were also analyzed through previous drilling report (UmiSan Report 2011/41), which allowed the analysis of lithological profiles in order to corroborate the geophysical data for the associated subsurface material.

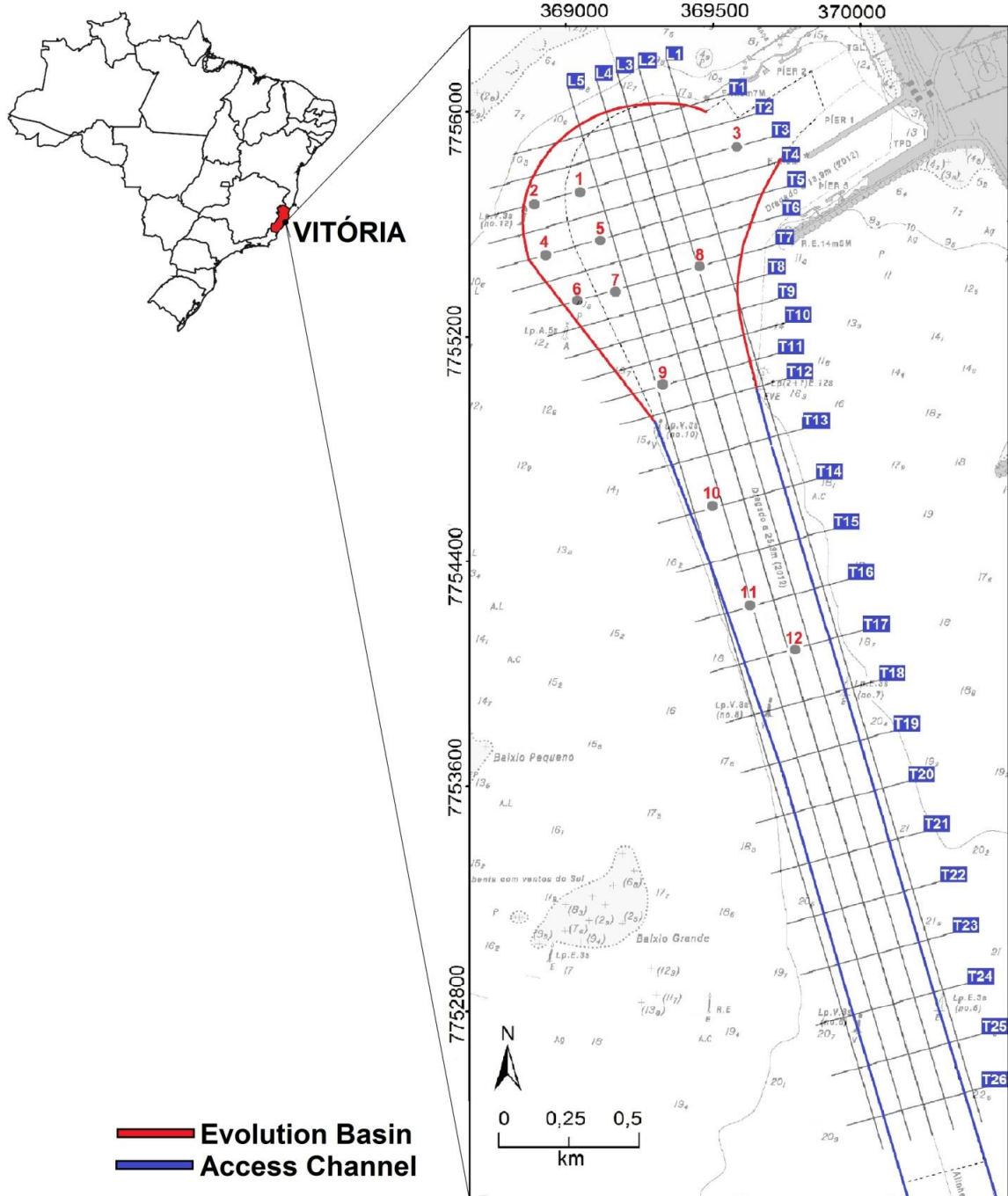


Figure 1 - Localization of the evolution basin, access channel, surveyed lines and collected seabed material.

The physical characteristics of the geological strata are interpreted by geoaoustic seismic data basically as a function of penetration and resolution values for individual geological strata.

The penetration is a function of the capacity of the seismic waves to reflect impedance contrast interfaces. Impedance contrast is related to the interface between two geological layers with distinct physical characteristics such as density, viscosity, compaction or porosity. Seismic profiles are capable of identifying such physical differences allowing interpretation as certain types of geological material, corroborated by in-situ data like borehole coring.

For this work the identification of the maximum depth of penetration for each equipment and frequency is conditioned to the visualization and consequent interpretation of the reflectors associated with the impedance contrasts identified by the acoustic seismic signals. The processed data of boomer and sparker were important to obtain the maximum visualization of the deepest points where the continuous reflectors associated with a single geological feature were present.

For sidescan sonar, this information is read in terms of backscatter strength. The comparison between the results obtained by different frequencies was statistically interpreted in terms of the capacities of penetration and resolution in function of the different geological materials that they reached and crossed. The seismic horizons were plotted for each of the reflectors in function of the different frequencies, the different penetration depth values were exported onto statistical software and boxplots were plotted, allowing quantifying the penetration capacity of each of the acoustic sources.

The frequency of the elastic waves produced by the acoustic transducers is inversely proportional to the energy required to produce such wave and how much will translate in penetration and resolution of the subsurface geological strata. High frequencies produce high vertical resolution and low penetration, whilst lower frequencies produce data with lower vertical resolution but with a higher penetration, therefore it is necessary more energy for its generation (Ayres Neto, 2000).

Vertical resolution is a measure of the ability to recognize closely spaced individual acoustic reflectors in depth and it depends on the wavelength (λ) of the produced elastic wave:

$$\lambda = v \times f$$

Resonant sources produce higher resolution records, allowing a greater definition of geological layers at shallow depths, just below the seabed, they use piezoelectric properties of some crystals to generate the acoustic signal and are usually pole-mounted, producing data with high geographical precision. The main advantages of resonant sources are operational ease, low maintenance cost, high repeatability rate, efficiency, high resolution and geographical accuracy.

Impulsive-type sources, such as boomers, transmits waves by mass acceleration, releasing energy stored in a capacitor and discharged on a flat spring connected to a vibrating plate, this source stands out for its great penetration capability. While Sparkers generate an electric discharge in the conductive medium and creates a high-power vapor

bubble and great emission power of wide frequency spectra (low and high frequencies), known for its low cost, high penetration, but with less repeatability and limited directivity.

These sources have great penetration capability, but their vertical resolution is much smaller when compared to the resonant sources and are towed behind the survey vessel, with varied cable layback, producing uncertainties in the geographic positioning of the produced profiles. These last sources produced acoustic waves, which were received and read through a single-channel hydrophone with several piezoelectric sensors arranged in a cable.

3. RESULTS

According to seismic data analysis, it was possible to observe that propagation and reflection showed distinct responses for the evolution basin and access channel regions, possibly due to distinct surface and subsurface geological features and correspondent physical characteristics (compaction, porosity, etc.)

Sediment analysis (Table 1) showed high content of mud on the seabed of all areas of the port at a content averaged at 90%. In the evolution basin, 20 to 30% of sand was found. Beneath the mud layer, a consolidated material was identified as sedimentary rocks and compacted clay by analysis of past data (UMISAN, 2008).

| SAMPLE | GRAVEL (%) | SAND (%) | MUD (%) |
|--------|------------|----------|---------|
| 1 | 0,09 | 22,48 | 77,43 |
| 2 | 4,87 | 29,87 | 65,26 |
| 3 | 0,91 | 93,15 | 5,93 |
| 4 | 0,21 | 6,28 | 93,51 |
| 5 | 0,00 | 0,88 | 99,12 |
| 6 | 0,02 | 71,18 | 28,80 |
| 7 | 0,00 | 12,99 | 87,01 |
| 8 | 0,03 | 65,27 | 34,70 |
| 9 | 0,00 | 0,53 | 99,47 |
| 10 | 0,00 | 6,39 | 93,61 |
| 11 | 0,00 | 0,17 | 99,83 |
| 12 | 0,01 | 0,32 | 99,68 |

Table 1- Sediment content.

The HF chirp was effective in visualizing a material with low reflection and low impedance contrast at its upper interface (water/unconsolidated material) and high contrast at its inferior interface (unconsolidated material/first reflector). The high impedance contrast is possibly associated to a non-consolidated material identified by sediment sampling as a package of mud with thicknesses of up to 1 meter, seen in the majority of the port's areas, with a high vertical resolution. Some geological features (discontinuous reflectors) are seen on the first meters of the sedimentary layers (Fig. 2.a).

Below the reflector associated with the clayey compacted material, there was practically no penetration regardless of the content of mud, preventing the identification of the thickness and spatial distribution of this clayey layer along the area. It is also possible to observe the event of an acoustic blanking (AB) and in the water column there is an event of a plume that can be associated to suspended particulate material (SPM)

dispersed through the water column.

As expected, the LF chirp was more effective in depth of penetration than the HF Chirp for the conditions of this research, only with lower vertical resolution. The mud layer is still quite visible and delineated throughout the evolution basin and access channel, as seen in Fig. 2.b), but it is no longer possible to see intra-layer details as in the higher frequency seismic source.

Previous drilling (Loureiro, 2013; UMISAN, 2008) allowed identifying these compacted sandstone and clay in different levels of lateralization of sandy and gravel sediments of the *Barreiras* Formation, corroborating the results obtained with sonar and seismic. It is possible to observe an acoustic masking feature in the surficial zone, possibly associated to a gas event, common in regions of organic matter deposition in mud layers (Fig. 2.b).

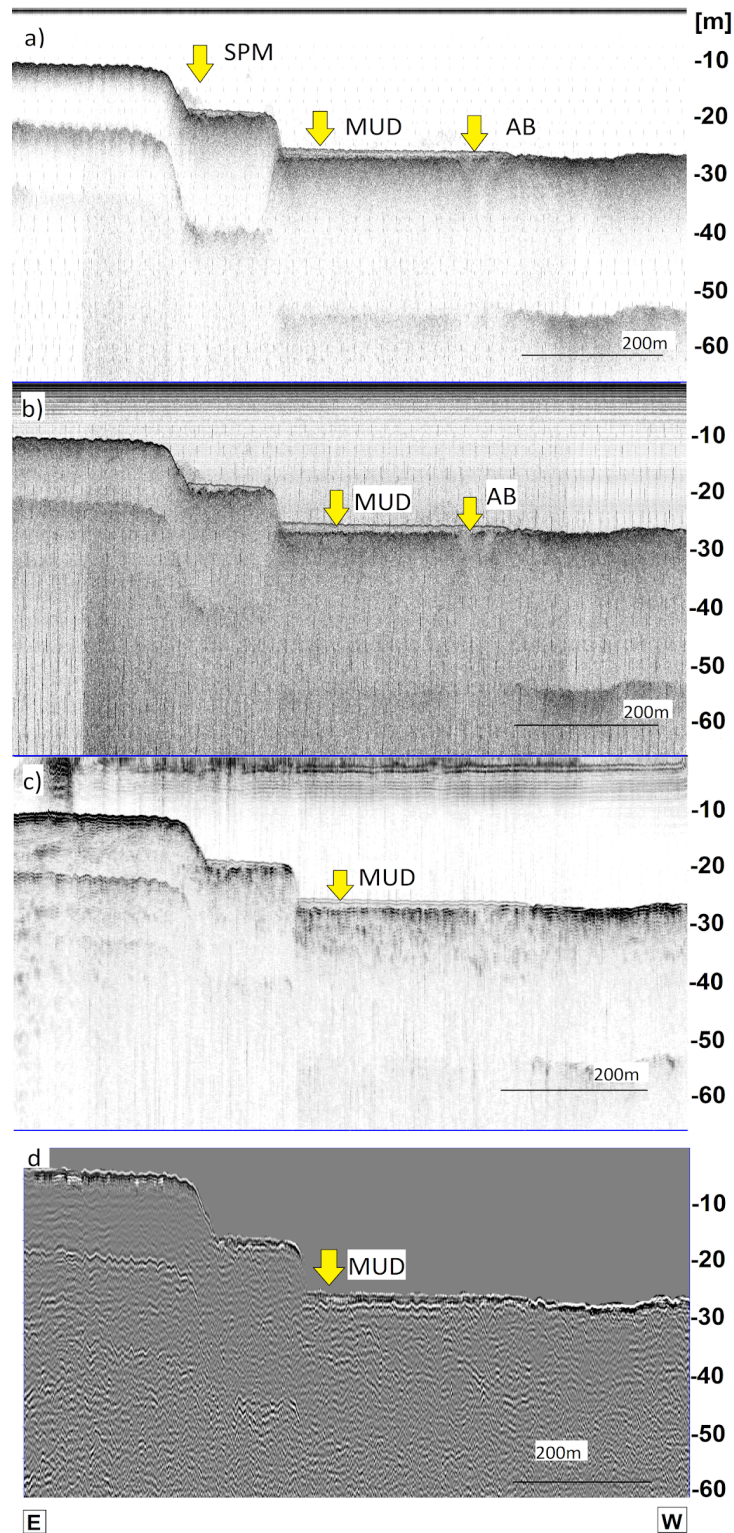


Figure 2 - Multifrequency seismic surveyed profiles on the access channel. (AB = Acoustic blanking)
a) HF Chirp, b) LF Chirp, c) Boomer, d) Processed Boomer.

The boomer source has greater penetration capacity than the Chirps, but lower vertical resolution. On the unprocessed profiles, it is possible to observe that the mud layer is visible in the evolution basin (Fig. 2.c) but it has a considerable decrease in resolution and the definition of the upper and lower limits of this layer becomes less specific in

access channel where, due to the irregular geometric nature of the reflector below the mud layer, several hyperbolic forms end up masking the features of the mud layer.

Processed boomer data suffers a considerable loss of resolution in the first few meters of the subsurface but shows discontinuous reflectors corresponding to deeper sandstone, which could not be visualized with any of the previous equipment with basic processing, highlighting the gain of visualization in reflectors in subsurface (Figs. 2.d), and later on figures 4.d and 5.d). The processed data helped defining the reflectors' horizons in deeper depths, therefore the evaluation of the penetration for each frequency could be made with more accuracy.

In the evolution basin, the SSS data (Fig. 3) is characterized by low backscatter strength (hereby designated as low reflection pixels pattern, LR), associated with mud, locally marked by the occurrence of high backscatter strength (hereby designated as high reflection pixels pattern, HR), with or without dredge marks, possibly associated with outcrops of sandstone or clay.

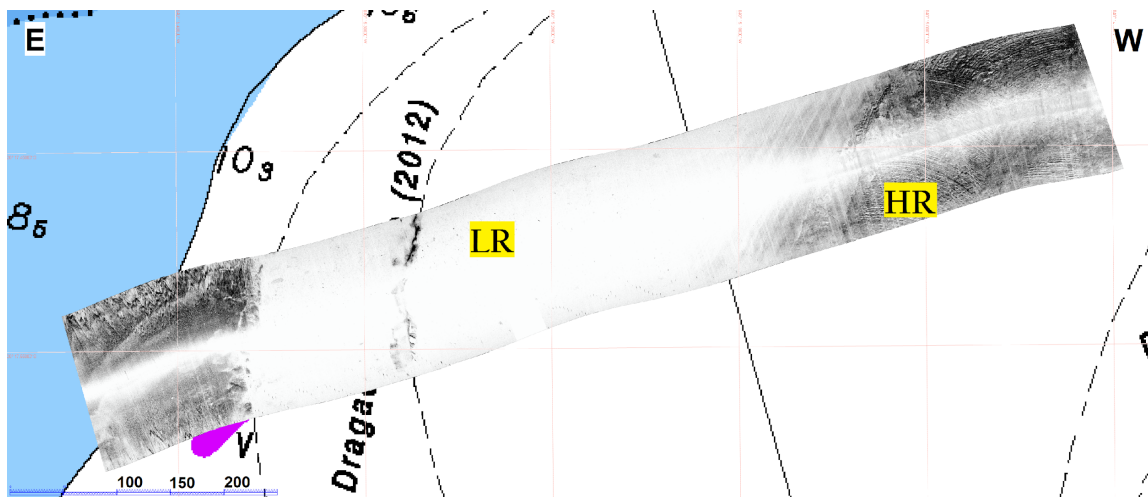


Figure 3 - HF SSS surveyed line on the evolution basin.

It was observed that the HF SSS allows high-resolution visualization of seabed shapes, cohesive sediments and morphological variations, whereas in the portion of the mud layer, the LF data demonstrates more detailed imagery.

In the access channel, the HF Chirp shows low penetration below the mud layer (Fig. 4.a), with evidence of compacted material of irregular geometry, interspersed by different impedance contrast materials, possibly associated with deposits of sand or sandstone (lateralized or not), dredged in previous projects. In general, lateritic horizons are irregular and have variable thicknesses, turning interpretation difficult because there is no well-defined pattern. The LF Chirp allows the visualization of a feature possibly related to a paleochannel (PC).

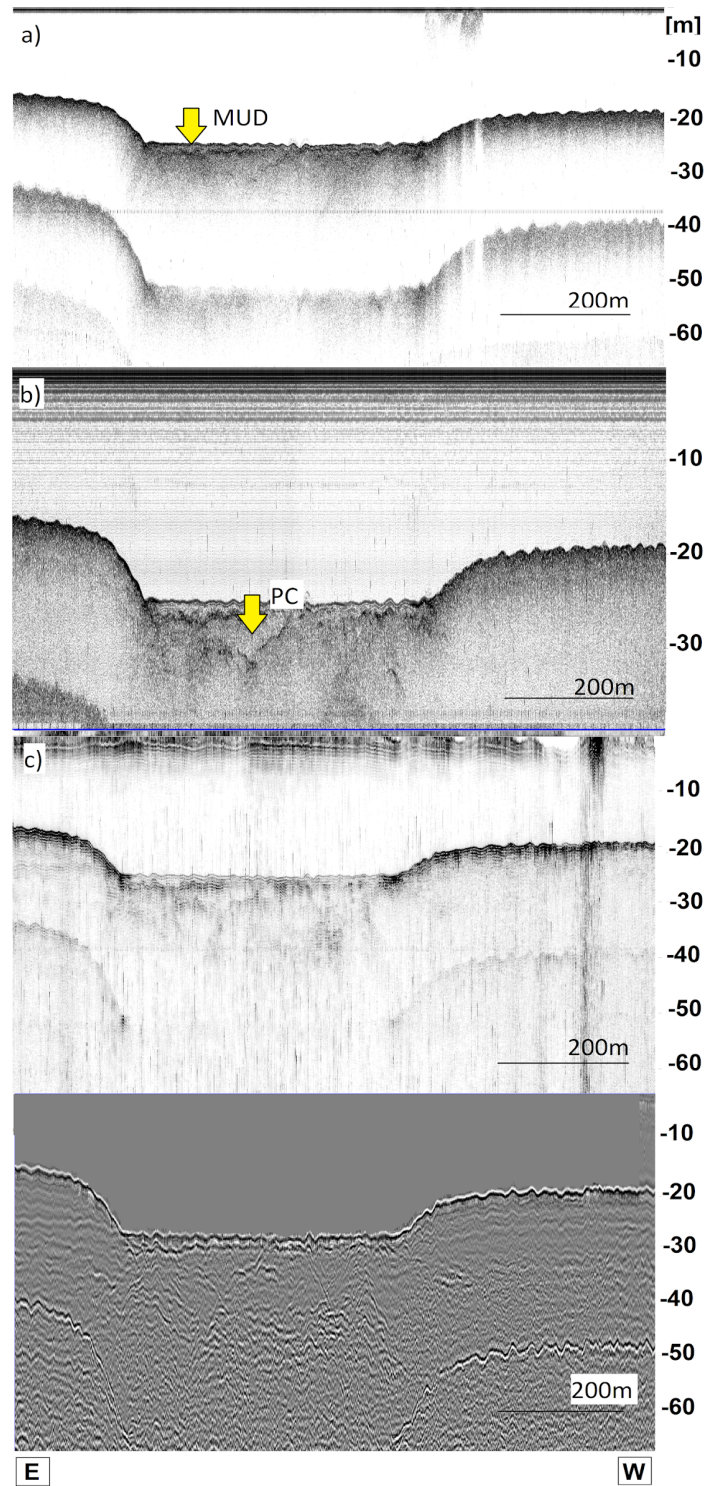


Figure 4 - Multifrequency seismic surveyed profiles on the evolution basin.
a) HF Chirp, b) LF Chirp, c) Boomer, d) Processed Boomer.

Irregular seabed geometry is seen on the seismic profile on the access channel as several diffraction hyperbola with penetration between 2 to 5 meters below the mud layer. Also in the access channel region, it is possible to observe the reflector associated with the outcrop of the crystalline basement (CB) (Fig. 5). In the access channel little content of sand was observed from sediment sampling, varying from 0 to 6%, such data corroborates with the penetration and reflection pattern seen on the seismic profiles.

The LF chirp (Figure 5.b) showed effectiveness in penetration, although the vertical resolution decreased from the higher frequency seismic source. The mud layer was visible throughout the whole area of the channel. Due to the geological content of the reflector below the mud layer, a higher penetration was possible in comparison to the evolution basin. The attenuation phenomenon is less intense in this region whilst deeper subsurface features are now more visible with better lateral continuity.

The boomer source showed greater penetration ability for that region than the LF and HF chirps but lower vertical resolution, as expected. The mud layer is visible with little resolution, similar to what is seen on the evolution basin. There is low penetration in the area indicating a sedimentary package less thick with the basement rock very close to the bottom surface (thicknesses between 0 and 2,5 m). It is possible to observe that the crystalline basement shows higher lateral continuity until depths of 50 meters.

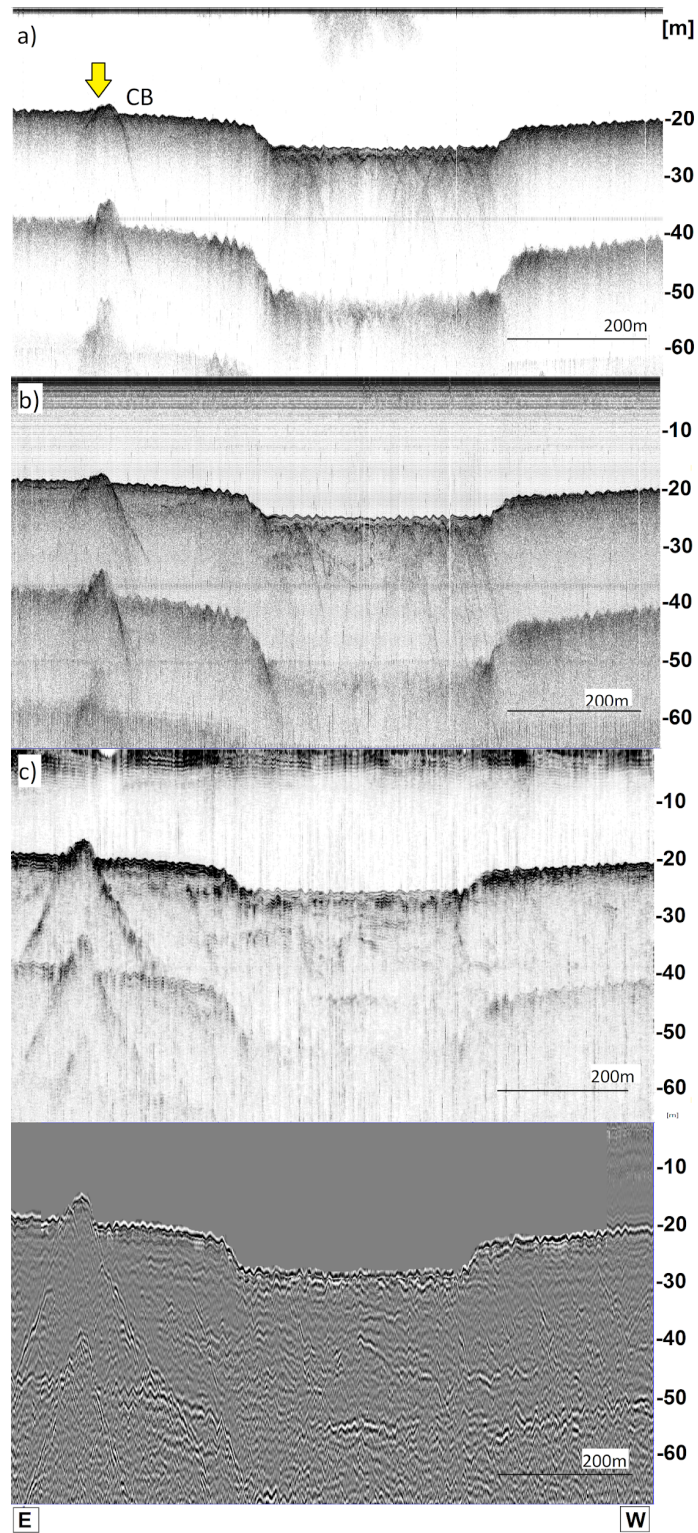


Figure 5 - Multifrequency seismic surveyed profiles on the access channel showing the crystalline basement outcrop. a) HF Chirp, b) LF Chirp, c) Boomer, d) Processed Boomer

As expected, the sparker source obtained a better ratio signal/noise than the boomer though lower resolution was seen. It is possible to observe that the non-processed profiles showed similar penetrations, but the effect of absorption and attenuation was smaller for the Sparker. In the evolution basin it is possible to observe that the mud layer was well delimited with little resolution, and the outcrops of consolidated material

associated with the first reflector are clear in both seismic source without good lateral continuity (Figure 6).

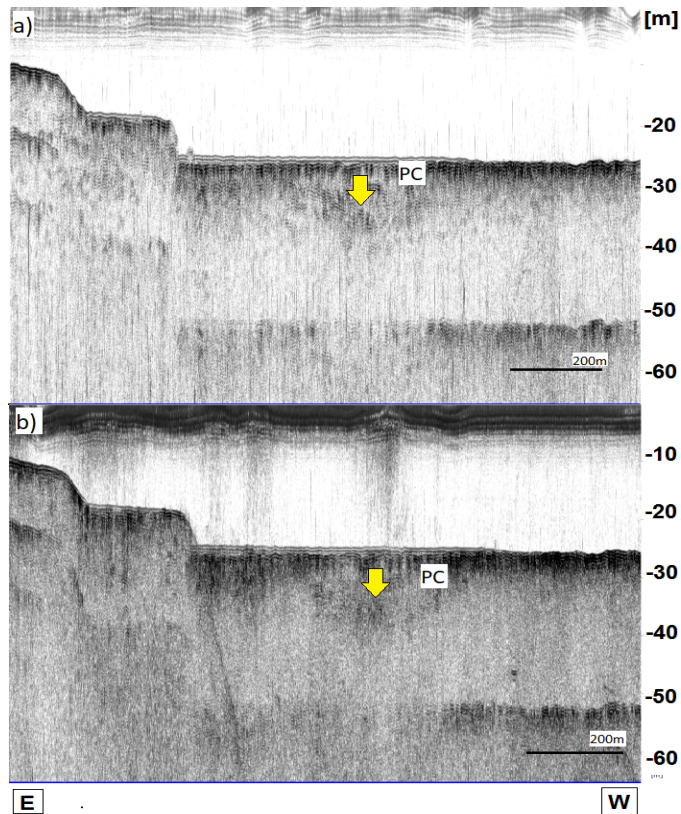


Figure 6 - Comparison between a) Boomer and b) Sparker surveyed lines at the exact same place.

In the navigation channel, for the sidescan sonar data it is possible to identify low backscatter (LR), (Fig. 7) with spaced occurrences of high backscatter (HR) sites, indicating the irregular seabed on which the layer of mud overlaps and also the possible sand mixed with mud. The material characterized as compacted clay is arranged in strata generally intercalated with sandy sediment, forming more consolidated surfaces that present a high contrast in the sonographic images.

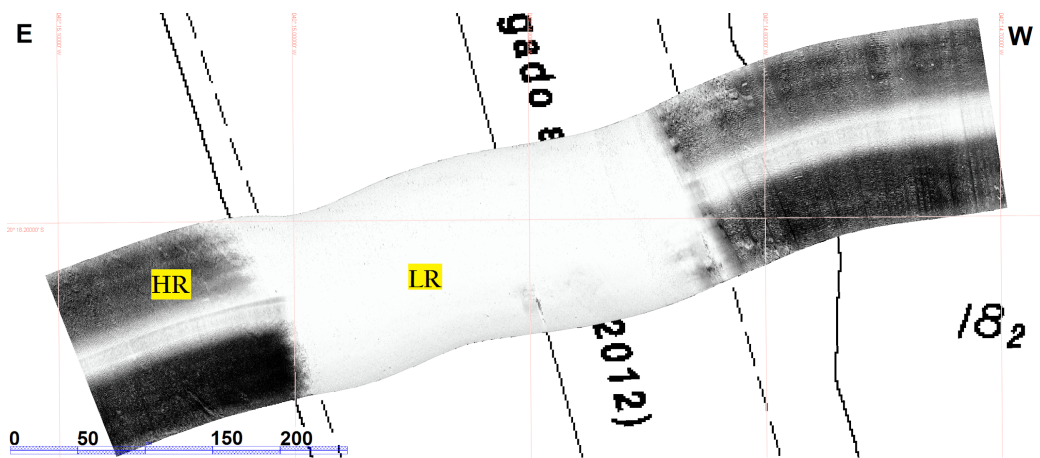


Figure 7 - HF SSS on the access channel.

The acoustic signal of suspended material can be observed through high attenuation and high frequency dispersion preventing the acoustic signal from effectively

reaching the seafloor. Fig. 8 shows a highly reflective and rough pattern (RUG), associated with crystalline basement outcropping.

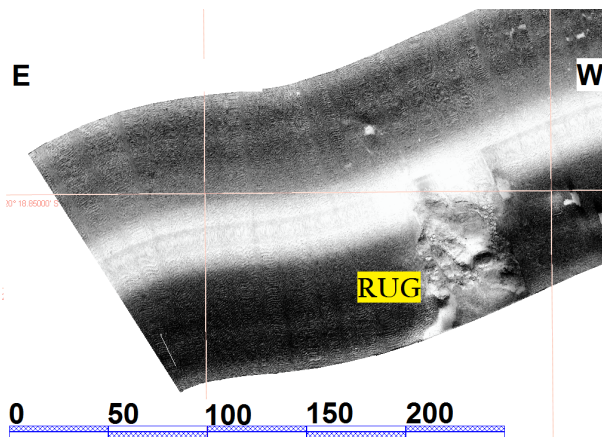


Figure 8 - HF SSS showing the crystalline basement outcrop.

3.1. SEISMIC AND SIDESCAN SONAR INTEGRATION

The seismic and sonar data integration and interpretation allowed the identification and mapping of sonographic echo characters, according to the classification proposed by Ayres Neto & Aguiar (1993) and modified to fit the peculiarities here seen. Classification is based on the acoustic signal reflection (backscatter) and dispersion intensities. SSS imagery were associated with seismic echo characters and then crossed with granulometry information and previous drilling reports allowing integration as seen in Table 2.

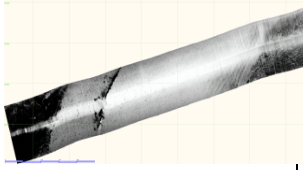
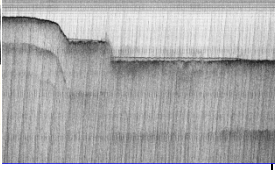
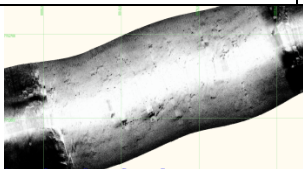
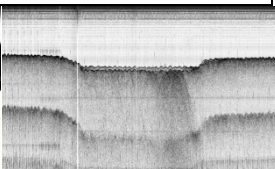
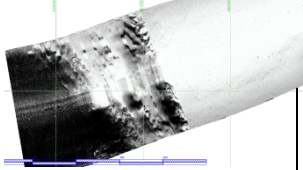
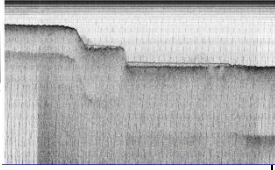
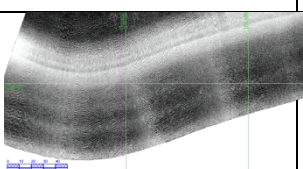
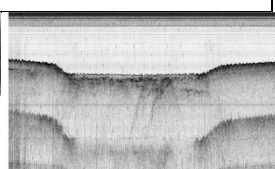
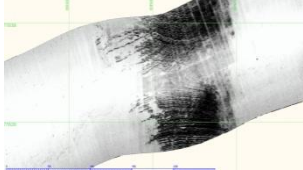
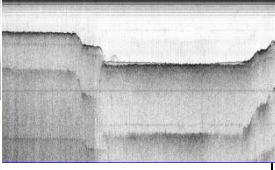
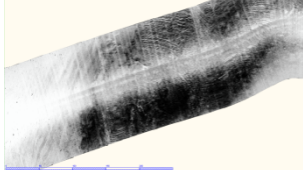
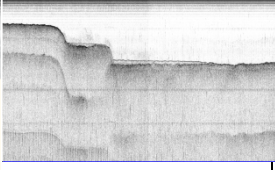
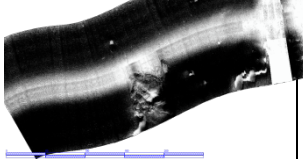
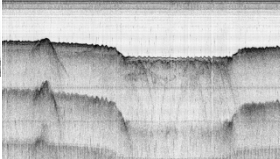
| Echo facies | Main Description | Backscatter Intensity Pattern | Seabed Material Type | Corresponding Sidescan Sonar Image | Corresponding Seismic Echocharacter |
|-------------|---|---|--|--|---|
| I | Low intensity backflow background surface followed by a highly reflective single subsurface reflector. No background shapes | Homogeneous pattern of low backscatter (LR) . | Mud |  |  |
| II | High penetration with subsurface reflectors. No background shapes or irregular background shapes. | Homogeneous pattern of low backscatter (LR) . | Mud/ Sandy-mud |  |  |
| III | High penetration, with subsurface reflectors. With the presence of irregular background shapes and background shapes. | Homogeneous pattern of low backscatter (LR) . | Muddy-sand |  |  |
| IV | Low penetration, no subsurface reflectors. With or without seabed shapes. | Seabed shapes pattern (SS) . | Sand |  |  |
| V | Low penetration, with subsurface reflectors. Irregular seabed shapes and masked hyperbolic reflections. | Heterogeneous pattern of high backscatter (HR) . | Presence of lateritic breastplates with sand. |  |  |
| VI | Low penetration, with subsurface reflectors. Irregular seabed shapes and masked hyperbolic reflections. | Heterogeneous pattern of high backscatter (HR) . | Presence of compacted clay with sand. (With or without dredging marks) |  |  |
| VII | Bottom surface highly reflective, with hyperbolic geometry and / or irregular. | Rugged pattern of high backscatter (RUG) . | Rocky outcrops or rock blocks. (With or without dredging marks) |  |  |

Table 2 - Correlation between geophysical and *in-situ* data.

4. DISCUSSION

From seismic and sonographic data, sedimentological categorization of the bottom material and the previous geotechnical drilling bulletins (UMI SAN, 2008 and 2011), it was possible to obtain a correlation between the geoacoustic information and the corresponding surface and subsurface materials. Depending directly on the frequency of each seismic source used. Therefore, it is necessary to discuss the factors that controlled the results of the acoustic responses and associate them with the respective acquisition frequencies, penetration and resolution.

The detection of the muddy deposit in was easily distinguishable for its low reflection index and backscatter. Different frequencies produce different degrees of

resolution and accuracy in determining the limits of the mud layer because of features such as compaction, the material of the first reflector below the mud layer, the presence of acoustic masking elements such as gas or irregular compacted morphological geometry and even elements present in the water column, as suspended particulate material.

Considering the observation of the seismic profiles, sidescan sonar imagery and the seabed samples, it is possible to associate areas of the seismic profiles where the interpretation led to the recognition of mud, consolidated material (compacted clay and sandstone) and the basement rock (crystalline basement). Comparison between the different seismic frequencies behavior in terms of penetration reach through each of the aforementioned strata was used to build boxplot graphs.

The HF Chirp was effective in identifying the layer of unconsolidated material identified by the high resolution with little penetration, whereas the LF Chirp was efficient in identifying the mud layer with lower vertical resolution but with better visualization of the underlying reflector (Figure 9.a).

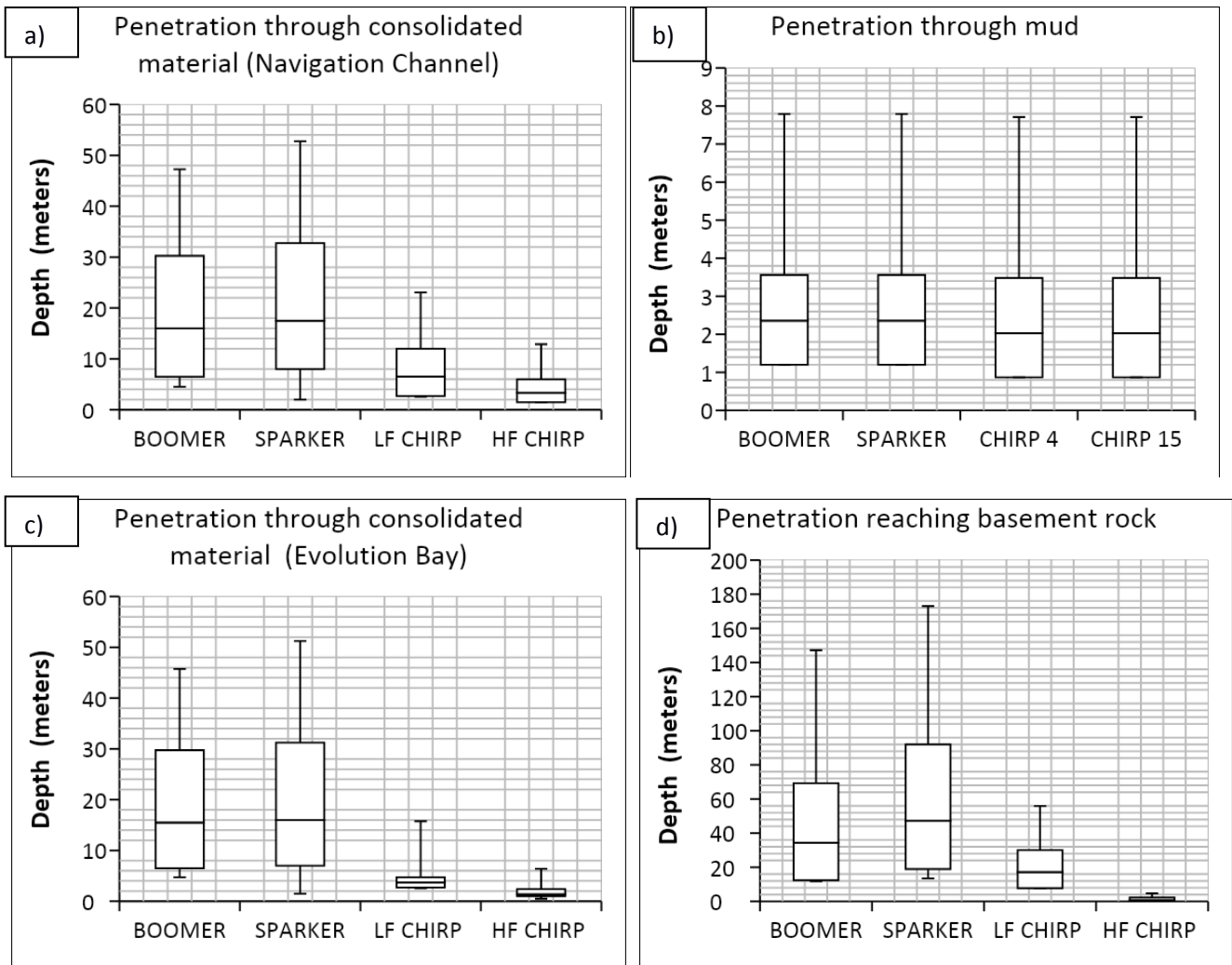


Figure 9 - Penetration through varied strata regarding each acoustic source.

Although the resonant acoustic sources have high vertical resolution, they are not able to differentiate the various degrees of compaction and density expected to be seen in a layer of mud deposited on the sea bottom due to constant silting processes (Carneiro, 2014). Some very high-resolution chirp source (20-50 kHz) might be able to observe such variations.

Mud undergoes a multi-stage deposition process, including fluid mud, classified by McAnally et al. (2007) as an aqueous suspension of highly concentrated fine sediments with density between 1080 and 1200 kg/m³, this variable density and viscosity are not identifiable by single-channel seismic or side-scan methods due to the impedance contrast between different degrees of non-continuous and vertical and lateral disordered compaction of the mud.

HF and LF chirps were not able to surpass the first reflector in the evolution basin, Figure 9.b, preventing the identification of the thickness and spatial distribution of the competent rock (sandstone or compacted clay) throughout that area, this phenomenon occurs due to the attenuation of the acoustic signal, upon reaching a high density and very irregular geometry substrate, considerably reduces, disperses and attenuates the pulse

energy and contributes to its disappearance, there being a high impedance contrast between the unconsolidated mud and the highly clayey competent rock (Kearey et al., 2002) (Figure 9.d).

The acoustic response associated with a high reflection seismic pattern extends throughout the evolution basin to the first reflector, inferring that the consolidated material below the first reflector possibly corresponds to compacted clay (*Tabatinga*) or sandstone with or without laterization. The *Tabatinga* was included in the morphological classification of the region of the Port of Tubarão by Albino et al. (2006) and also observed by Carmo (2009), being described as formed by laminated sandy sediment, compacted of whitish and reddish color.

These clays are unique in that they do not disperse or absorb the energy of the seismic waves due to their consolidated or semi-consolidated state. Instead they reflect the seismic signal almost completely. This acoustic facies is very similar to acoustic blankets or other highly concentrated gassy sediments.

For the HF and LF Chirp data it is possible to compartmentalize the port areas as a function of the difference in subsurface penetrations, as seen on the chirp profiles, the penetration on the evolution basin and the access channel differ on the absorption intensity and penetration capacity due to the presence of consolidated clayey material on the evolution basin and sedimentary rocks on the access channel.

Another determining factor for the HF signal return pattern was the highly irregular and disturbed bottom morphology related to dredging activities, easily visible in side-scan sonar images, and influencing the quality of the seismic profile, making it difficult to identify the first reflector corresponding to the sandstone or *Tabatinga* by the appearance of numerous diffraction masking hyperbola. This type of echo shows regular, very intense overlapping hyperbola with little varying vertex elevations and very prolonged echo without sub-bottom reflectors. Each hyperbola is generally less than 3 m in relief and 1-2 m in wavelength. These hyperbolas are suggestive of basement highs or outcrops and have no relationship to near-bottom sedimentation processes (Damuth, 1980).

Exposed sandstone rocks, mainly observed on the evolution basin, may represent hazardous dredging areas as the laterite and diagenetic process creates a "hard cover" in the sandstone and does not follow any depth pattern, attenuating the acoustic signal and causing the higher frequencies to not penetrate below this layer and the lower frequencies lose significant lateral continuity, making it difficult to identify the seismic reflectors.

It was observed that chirp sources are conditioned by sediment type and mud content, so the change in particle size of sand to mud decreases the penetration. Baldwin et al. (1985) found higher correlations between acoustic impedance and density than acoustic impedance and grain size, results that are similar to the data set presented here, including the statistical analysis. The LF Chirp was 46% more effective in penetration reaching the consolidated sediment than the HF Chirp while the LF Chirp achieved 96% more penetration as seen in Table 3.

| BASEMENT ROCK | | | | |
|--|-----|-------|-------|--------|
| DIFFERENCE IN PENETRATION BETWEEN TRANSDUCERS (%) | | | | |
| | BMR | SPRKR | CHP 4 | CHP 15 |
| BMR | 0 | 20 | 61 | 96 |
| SPRKR | 20 | 0 | 68 | 98 |
| CHP 4 | 61 | 68 | 0 | 91 |
| CHP 15 | 96 | 98 | 91 | 0 |

| CONSOLIDATED ROCKS | | | | |
|--|-----|-------|-------|--------|
| DIFFERENCE IN PENETRATION BETWEEN TRANSDUCERS (%) | | | | |
| | BMR | SPRKR | CHP 4 | CHP 15 |
| BMR | 0 | 0 | 25 | 60 |
| SPRKR | 0 | 0 | 25 | 60 |
| CHP 4 | 25 | 25 | 0 | 46 |
| CHP 15 | 60 | 60 | 46 | 0 |

Table 3 - Penetration comparison, in percentage, of each source considering consolidated subsurface material.

Boomer and Sparker were able to penetrate through subsurface layers Figure 9.b and 9.c) by identifying the thicknesses of the reflectors associated with the consolidated material in depth, but with different resolutions. The processed data showed the mud layer with lower resolution but with efficient penetration, reaching up to 60m Figure 9.a). There was a discrepancy of mud penetration values compared to the Chirps due to the uncertainty of the limits of the layer generated by the weak vertical resolution in the first few meters due to the filtering, emphasizing that the LF equipment is not ideal for imaging the seabed surface.

Boomer presented an optimal penetration and resolution, regardless of the sediment background and content of mud found on the seabed, but is affected by various noise (Ehrenberg & Torkelson, 2000) and attenuation by the mud and sand interleaved. More practically, the impedance contrast between sand layers and mud layers may only be sufficiently visible to 0.6s two-way time due to the similar acoustic impedance of mud and sand below that depth. At shallow burial depths, sediments undergo large changes in response to gravitational compaction, but these changes are lithology dependent. Mud is deposited at the seafloor with higher porosity (lower density) and exhibit lower velocity than sands. Below the seafloor, the porosity of mud reduces much more quickly with depth than sand.

Seismic records revealed lower vertical resolution and an increase in reflector thickness as the energy applied to the system increased. According to Applied Acoustics (2009), the higher the energy imposed, the lower the frequency spectrum amplitude and the lower the main frequencies. The theoretical resolution is about a quarter of the wavelength independent of the medium of propagation (Sheriff and Geldart, 1995). The sparker, whose energy output and lower signal-to-noise ratio was more efficient in resolution than Boomer, showed 20% more penetration than Boomer in the layers of consolidated material (Figure 9.d).

These results allow affirming that the penetration of this type of source is more conditioned with the faciological characteristics along the vertical profile in depth, than the faciology of the seabed. The higher the penetration, the lower is the influence of the surficial sediment in the penetration.

After processing, the reflectors near the surface suffered a great loss of vertical resolution, practically disappearing, unlike the deeper reflectors, which can be observed at even greater depths. This is because the increase in deep propagation contributes to the fact that the lower frequencies are dominant due to the effects of the absorption of the higher frequencies near the surface (Kearey et al., 2002).

On the HF and LF Chirp profiles, it is observed cloudy acoustic turbidity in the upper water layer. These features can be caused by point scatters in the water column such as matter in suspension. The high SPM meant the degradation of the SSS signal through the water column above the mud deposit, most notably in the higher frequency (900 kHz), preventing the signal from reaching the seafloor. In the LF SSS image, the water column displays as a translucent dark brown color, but can be easily distinguished from the seafloor. However, in the HF SSS image, the water column is a solid brown color, and is practically indistinguishable from seafloor. In the seismic data (Figure 3.a), it is possible to see the features associated with SPM, present mainly in the areas with great thickness of mud resuspended by the passage of large vessels.

The LF SSS shows discrete backscatter differences of the varying sediment textures on mud, which cannot be seen with the HF due to the attenuation and dispersion by the SPM. The LF signal seems to pass less affected by suspended particulate matter (SPM), most likely due to its wave frequency (455 kHz), high concentrations of SPM have a negative impact on the mapping capabilities of HF SSS.

The comparison between Boomer, Sparker and HF and LF Chirp sources shows a resolution/frequency relation. Not-so-large or prominent features in the seabed are seen with good resolution in the HF Chirp, more diffuse in the LF Chirp and finally Boomer and Sparker had difficulties in detailing this feature due to their wavelength and low signal directivity. Acoustic sources with greater directivity, such as resonant have a greater power to discriminate these minor features.

The multifrequency approach was useful for calculating the thickness of the mud layer, corroborated by the reflection patterns identified by the SSS and seen in the backscatter compartmentalization map (Figure 10). The figure shows the distribution of acoustically transparent and possibly fluid mud, concentrated throughout the access channel and evolution basin.



Figure 10 - SSS backscatter pattern compartmentation.

In terms of penetration, the comparison of all frequencies shows that Boomer and Sparker when reaching higher depths of the surface of consolidated rocks had the same penetration performance, being 60% more efficient than the HF Chirp and 25% more efficient than the LF Chirp. For the crystalline basement in deeper portions, Boomer was 96% and Sparker was 98% more efficient than the HF Chirp, in comparison to the LF Chirp, they were 61% and 68% more efficient, respectively. The synthesis between penetration and resolution for all frequencies in all port areas as a function of surface or subsurface material can be seen in Table 4.

| Seismic Source | Site | Material | | | | | | | |
|----------------|------|----------|-------------|-------------|-------------|-------------|-------------|------------|-------------|
| | | Mud | | Sandstone | | Tabatinga | | Bas. Rock | |
| | | P | R | P | R | P | R | P | R |
| HF Chirp | EB | Green | Green | Red | Green | Red | Green | Red | Green |
| | NC | Green | Green | Light Green | Green | Light Green | Green | Light Pink | Green |
| LF Chirp | EB | Green | Light Green | Red | Light Green | Red | Light Green | Red | Light Green |
| | NC | Green | Yellow | Green | Yellow | Green | Yellow | Yellow | Yellow |
| Boomer | EB | Green | Red | Light Green | Light Pink | Light Green | Light Pink | Yellow | Yellow |
| | NC | Green | Red | Green | Light Pink | Green | Light Pink | Green | Yellow |
| Sparker | EB | Green | Red | Light Green | Yellow | Light Green | Yellow | Yellow | Light Green |
| | NC | Green | Red | Green | Yellow | Green | Yellow | Green | Light Green |

| SSS Frequency | Site | Material | | | | Label |
|---------------|------|---------------------|-------------|-------------|-------------|-----------|
| | | Mud | Sandstone | Tabatinga | Bas. Rock | |
| | | Resolution Coverage | | | | |
| 500 kHz | EB | Green | Light Green | Light Green | Light Green | Very high |
| | NC | Green | Light Green | Light Green | Light Green | |
| 900kHz | EB | Light Green | Green | Green | Green | High |
| | NC | Light Green | Green | Green | Green | |

| Label | Color |
|-----------|-------------|
| Very high | Green |
| High | Light Green |
| Average | Yellow |
| Low | Light Pink |
| Very Low | Red |

Table 4 - Evaluation of the penetration and resolution for all frequencies according to each geological material. P stands for penetration and R for resolution

5. CONCLUSION

On muddy surface intervals, reflections were weak due to a lower acoustic impedance contrast and the penetration of the acoustic wave was higher, due to the lower signal attenuation. The identification of mud occurrence was possible in all frequencies in both seismic and SSS data, although each frequency had particularities regarding resolution and penetration. The seabed material sampling analysis confirmed the existence of the fluid mud, however the identification of the fluid phase through the acoustic methods here presented was not possible once these equipment do not identify density and viscosity. It is also evident that for the identification of the fluid mud, a more detailed rheological acoustic study is necessary, such as in-situ evaluation. That understanding leads to the following chapter.

Outcrops of consolidated strata were observed in both seismic and SSS data, it was possible to associate such material with sandstone or compacted clay. The frequencies of 2-8kHz and 10-18kHz were not able to reach to deeper consolidated strata horizons in the evolution basin while in the SSS it was possible to identify dredging marks. For this situation the multifrequency approach was especially useful because boomer and sparker data allowed the visualization below that reflector, whereas chirp was not able to, as expected.

Chirp-type sources are usually pole-mounted and have accurate geographic positioning whereas cable towed sources such as boomer and sparker show small localization variations. That being an important factor to consider in dredging project. The multifrequency approach is effective because it corroborates geographic information from

several sources and produces an ideal product that allows the analysis of high resolution (high frequency) and subsurface data at higher depths (low frequencies).

The 900kHz SSS images were effective in visualizing surface features such as consolidated rocks and seabed shapes. Whereas the 500kHz showed better visualization features associated with mud and suspended particulate material. Showing the benefit of using multifrequency SSS.

The maps and statistical graphs produced illustrate how the multifrequency acoustic approach can be useful in building a complete and accurate mapping of port environments, from the point of view of resolution and penetration, ensuring maximization of product quality and minimizing operational costs. A total observation of the surface and subsurface allows a better understanding of the local geology and sedimentary processes, important for the full development of any port project.

The use of a spectrum of frequencies was proven to be quite effective so that the high seismic frequencies mapped the first centimeters and meters of the seafloor, identifying mud layers, while the lower frequencies reached deeper consolidated strata, identifying sedimentary layers to the crystalline basement. The dual frequency side-scan sonar identified different backscatter strength associated with different morphology and lithologies.

The more a fair amount of different frequencies and acoustic techniques are applied, the more is known about the environment studied, resulting in minimizing costs and a better mapping for dredging activities. It is crucial to choose the correct techniques to get the best results, since each device has its own frequencies and operational requirements. The quality of the data also depends on site-specific physical parameters.

6. REFERENCES

- Albino, J.; Girardi, G.; do Nascimento, K. A. 2006. *Espírito Santo*
- Amos, C. 1996. A Rapid Technique for the Determination of Dry Sediment Mass from Saturated Marine Sands: ERRATUM. *SEPM Journal of Sedimentary Research*. Vol. 66. 10.1306/D4268473-2B26-11D7-8648000102C1865D.
- Atherton, M. W. 2011. Echoes and Images, The Encyclopedia of SideScan.
- Ayres Neto, A.; Aguiar, C. K. V. 1993. *Interpretação de reflexões de Side-Scan Sonar: uma proposta de nomenclatura e padronização de métodos, Anais do Congresso Internacional de Geofísica* RJ 399–403.
- Ayres Neto, A. 2000. *Uso da sísmica de reflexão de alta resolução e da sonografia na exploração mineral submarina, Revista Brasileira de Geofísica* 18 (3) 241–256.
- Bastos, A. C.; Costa Moscon, D. M.; Carmo, D.; Baptista Neto, J. A.; Quaresma, V.S. 2014. Modern sedimentation processes in a wave-dominated coastal embayment: Espírito Santo Bay, southeast Brazil. *Geo-Marine Letters* , v. 35, p. 23-36.
- Baldwin, C., Kenneth & R. LeBlanc, Lester & J. Silva, Armand. 1985. An analysis of 3.5 kHz acoustic reflections and sediment physical properties. *Ocean Engineering - OCEAN ENG.* 12. 475-492. 10.1016/0029-8018(85)90021-6.
- Blondel, F., 2009. *The Handbook of Side Scan Sonar*. Praxis Publishing Ltd, Chichester UK. 344pp.
- Carmo D. A. 2009. *Mapeamento Faciológico do Fundo Marinho como Ferramenta ao Entendimento da dinâmica sedimentar da Baía do Espírito Santo, Vitória (ES)*, UFF, Niterói, RJ.
- Carneiro, J. C.; Fonseca, D. L.; Vinzon, S. B.; Gallo, M. N. 2017. Strategies for Measuring Fluid Mud Layers and Their Rheological Properties in Ports, *Journal of Waterway, Port, Coastal, and Ocean Engineering* 143 (4) 04017008.
- Damuth, J. 1980. Use of high-frequency (3.5–12 kHz) echograms in the study of near-bottom sedimentation processes in the deep-sea: A review. *Marine Geology - MAR GEOLOGY.* 38. 51-75. 10.1016/0025-3227(80)90051-1.
- Ehrenberg J. E.; Torkelson C.; Thomas, F.M. 2000. Slide (chirp) signals: A technique for significantly improving the signal-to-noise performance in hydroacoustic assessment systems, *Fisheries Research* 47 (193-199) 10–1016.
- Fish, J. P.; Cara, H. A.; *Sound Underwater Images*, 1990, pp. 1–188, Sound Underwater Images.
- Gallea, C. G., Souza, L. A. P., R. Bianco, 1989. *A geofísica marinha de alta resolução: características e aplicações. In: Congresso Internacional*, Vol. 1.
- Jones, E.J.W. 1999. *Marine geophysics*. Baffins Lane, Chichester, John Willey & Sons Ltd. Inc. 466p.
- Keary, P.; Brooks, M.; Hill, I. 2002. *An Introduction to Geophysical Exploration*, Blackwell Publications, Oxford.
- Loureiro, D. V.; Bastos, A. C. 2011. *Comparação entre Fontes Sísmicas de Alta Resolução*, in: 12th International Congress of the Brazilian Geophysical Society & EXPOGEF, Rio de Janeiro, Brazil, Society of Exploration Geophysicists and Brazilian Geophysical Society, 2011, pp. 1920-1925.
- Loureiro, D.V. 2013. Estudo de caso da dragagem do porto de tubarão (Vitória-ES): Utilização integrada de dados geofísicos e geotécnicos. Master's Thesis. Programa de Pós Graduação em Oceanografia Ambiental, UFES.

- McAnally, W. H.; Friedrichs, C.; Hamilton, D.; Hayter, E.; Shrestha, P.; Rodriguez, H.; Sheremet, A.; Teeter, A. 2007. Management of fluid mud in estuaries, bays and lakes. I: Present state of understanding on character and behavior, *Journal of Hydraulic Engineering* v.133, n.1.
- Mosher, D. C.; Simpkin, P. G. 1999. Status and Trends of Marine High-Resolution Seismic Reflection Profiling: Data Acquisition, *Geosciences Canada* 26. 174–188.
- Quaresma, V. S.; G.T.M. Dias & J.A. Baptista Neto. 2000. Caracterização da ocorrência de padrões de sonar de varredura lateral e sísmica de alta frequência (3,5 e 7,0 kHz) na porção sul da Baía de Guanabara. *J. Rev. Bras. Geof.*, 18(2):201-214.
- Souza, L. A. P. 2006. *Revisão crítica da aplicabilidade dos métodos geofísicos na investigação de áreas submersas rasas, Doctorate's Thesis*. 311.
- Souza, L. A. P.; Bianco, R.; Tessler, M.G.; Gandolfo, O. C. B. 2007. *Investigações geofísicas em áreas submersas rasas: qual o melhor método?* 10th International Congress of the Brazilian Geophysical Society.
- Souza, L. A. P. 2008. *A investigação sísmica de áreas submersas rasas; parte 1: fundamentos e demandas*, SBGf Bulletin 2 11–29.
- Souza, L. A. P.; Mahiques, M. M. 2009. *Geofísica Marina Aplicada al Estudio de los Riesgos Geológicos Litorales, Métodos en Teledetección Aplicada a la Prevención de Riesgos Naturales en el Litoral* 297.
- Souza, L. A. P.; Azevedo, A. A.; Silva, M. D. 2013. Side Scan Sonar Applied to water reservoir, in: 2013 IEEE/OES Acoustics in Underwater Geosciences Symposium, RIO Acoustics 2013,
- Sheriff, R. E.; Geldart, L. P. 1982. *Exploration Seismology*, Volume 1.
- Telford, W. M.; Geldart, L. P.; Sherif, R. E. 1990. *Applied Geophysics*, 2nd Edition, Cambridge University Press.
- Tóth, T.; Vida, R.; Horváth, F.; Simpkin, P. 1997. Shallow-water single and multichannel seismic profiling in a riverine environment, *The Leading Edge* 16 (11) 1691–1695.
- UMI SAN. 2008. *Levantamento Sísmico no Porto de Tubarão – ES*. Relatório Técnico nº 52 -2008. 28 p.
- UMI SAN. 2011. *Levantamento Sísmico de Reflexão. Relatório Técnico nº 41 - 2011*. 29 p.

CHAPTER 4

GEOACOUSTIC AND DENSITOMETRIC METHODS AS A TOOL FOR ASSESSING NAUTICAL DEPTH

ABSTRACT

Fine sediment deposition can pose a threat to navigation channels due to possible reductions in nautical depth, demanding seasonal dredging activities. Dredging and safety navigation are the most important issues regarding ports management. Although when the mud layer is fluidized, it is not considered part of the consolidated seabed, as it does not show mechanical resistance, leading to a decrease in the need for dredging and the possibility for navigating in fluid mud (Kineke & Sernberg, 1995). In this perspective, the nautical bottom concept was developed and implemented in several major ports. Singlebeam dual-frequency bathymetry methods (24, 33 or 38 and 200 kHz) are commonly used to build nautical charts, to define the acceptable under keel clearance and silted volumes and to perform dredging activities. However, the fluid mud layer cannot be reliably detected by traditional acoustic methods due to inconsistent penetration through the unconsolidated sediment. This work aims to contribute to the understanding of the acoustic response on muddy areas and its relation to actual density values within the fluid mud layer through a combination of *in situ*, acoustic, and direct density measurements as well as laboratory tests at the Port of *Tubarão* (Vitória/Brazil).

Keywords: nautical depth, hydrography, single-beam echosounder, densitometer, ports, harbors, dredging, navigability, fluid mud, shallow-water, geoaoustics.

1. INTRODUCTION

Acoustic methods are widely used for mapping navigation risks and aiding dredging activities. In port environments, the navigation channels and evolution basins present high siltation rates and mud formation with variable rheological characteristics and hydrodynamic processes (Dyer, 1986 and Whitehouse et al., 2000).

Fluid mud is known by its high-concentration aqueous suspension of fine-grained sediment in which the settling process is relatively hindered by the proximity of sediment grains and flocks. The bonds formed are not strong enough, leading to a persistent suspension (McAnally et al. 2007a). Therefore it has no mechanical resistance and can be mobile or stationary and is not considered part of the consolidated seabed (Kineke and Sternberg, 1995). Its concentration can vary from 1080 to 1200 kg/m³, according to McAnally et al. (2007a, 2007b).

Continuous mud deposition may be a threat to navigation and might cause considerable reductions in nautical depth (Mehta & Dyer, 1990; Parker & Lee, 1979; Sills, 1994; Wolanski et al., 1992 and Whitehouse et al., 2000).

Ports must guarantee safe passage of ships to and from its waterways. Thus, for sites where high siltation rates persist, this service leads to elevated maintenance costs and millions of tons of sediment are dredged from ports around the world for this purpose (Fontein and Byrd, 2007; Welp and Tubman, 2017).

Dredging operations are massively costly and result in environmental issues related to resuspension of contaminated sediments and reject sites. Also, in muddy areas there is the generation of internal waves when vessels navigate too close or through the water-mud interface. Those undulations can restrain the controllability and maneuverability and negatively affect the efficiency of the rudder and propeller (Wurpts, 2005; McAnally et al. 2007a).

Geoacoustic methods are commonly used in port areas for monitoring, determining the navigable depth and for evaluating the volumes of silted material to be dredged. The presence of fluid mud on the seabed is characterized by a sharp variation in the mass volumetric density gradient along the water column (Mehta, et al., 2014; Schettini et al., 2010). The consolidation state of the cohesive sediment can be described by a vertical profile built with geoacoustic methods (Carneiro et al., 2017; Fontein & Bird, 2007 and Kirby et al., 1980).

However, the rheological state of the mud may present different acoustic responses in both single-beam dual frequency echosounders and seismic profilers (Carneiro, 2017; Wurpts, 1998; Madson & Sommerfield, 2003). Rheology is an important feature for understanding the deformation and flow of geological materials under the influence of an applied stress (Schettini et al., 2010). Density assessment is closely related to the acoustic impedance and frequency emitted by the acoustic source (Fonseca et al., 2018; Granboulan et al., 1989).

The frequency produced by the seismic sources is directly proportional to the attenuation ratio, whilst the depth acquired by the bathymetric method in fluid mud is a function of the sharpness of the density gradient of the fluid mud (Carneiro, 2017; Timothy et al., 2017).

High frequency echo sounders (200 kHz and higher) can reflect off the water/low-density semi-fluid muds interface (i.e., the lutocline), whereas the low frequency echo sounders (24, 30, 33 or 38 kHz) can reflect off a density gradient (or density gradients) within the fluid mud layer (Clayes, 2006; USACE, 2002 and 2013). This situation can lead to misinterpretation of the seabed conditions in shallower sections leading to unnecessary dredging actions (Buchanan, 2005).

Although dual-frequency echo sounder systems have been used to assess mud layer depths and thicknesses over the years (Madson and Sommerfield 2003; Schettini et al. 2010; Shi et al. 1999), these indirect methods do not determine properly the navigability on muddy seabed (Carneiro et al., 2017) because the suspended sediment concentration within the fluid mud layer can return false bottom records to acoustic systems. Therefore these methods must be coupled with *in situ* methods, seabed material sampling and laboratory tests.

If there is a steady increase of density in the seabed, PIANC (2008, 2014) recommends caution in the use of an echo sounder. For the same conditions, the US Army Corps's Hydrographic Surveying Manual, USACE (2013) states that depth records when surveying over fluid mud surfaces cannot be interpreted properly unless other *in-situ* correlating information is obtained in order to implement the nautical bottom (Buchanan, 2005).

The nautical bottom concept is currently defined as: "The level where physical characteristics of the bottom reach a critical limit beyond which contact with a ship's keel causes either damage or unacceptable effects on controllability and maneuverability" (PIANC, 2014; Teeter, 1992).

This concept allows navigating through mud when the low strength of the fluid mud does not represent risks for the vessel and negative under keel clearance (UKC) can be considered, enabling navigation through layers with densities of up to 1,350 kg/m³ (Figure 1). The need for maintenance dredging can be postponed or reconsidered (Fontein & Byrd, 2007; Kirichek et al., 2018; Wurpts, 2005).

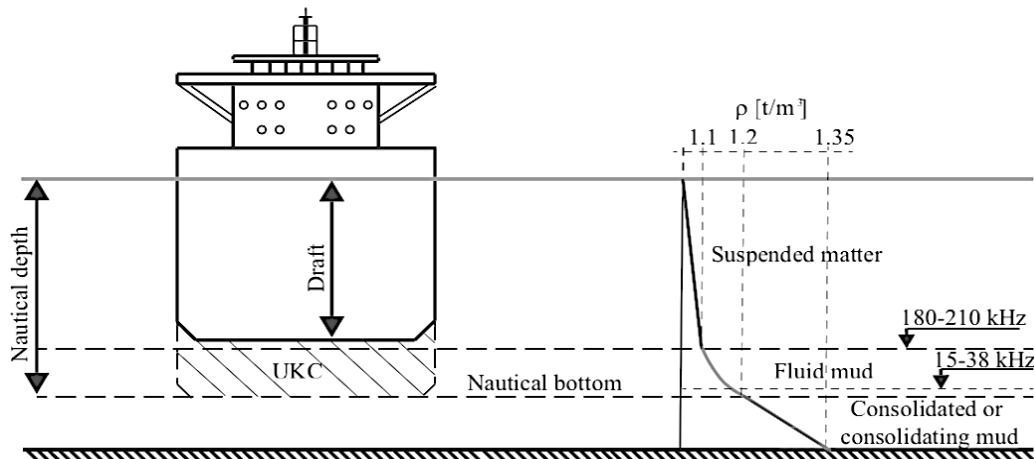


Figure 1 - The nautical bottom concept. Modified from Nederlof, L. (1978).

Navigation in fluid mud has not yet been well documented in Brazil, although this feature is seen in many ports in the country, such as in Rio Grande (RS), Ilha Grande (SP), Rio Potengi (RN) and at the Amazon River delta (AM). Nonetheless, nor the maritime authority (Brazilian Navy) neither the Ports authority (Coastal and Ports Directory) have yet set normative understanding for navigation through fluid mud (Noernberg & Soares, 2007). Many European ports have adopted navigation on fluid mud (i.e.: Rotterdam and Zeebrugge) and have been developing research since 1980 (Wurpts, 2005; Mehta, 1987).

However, the Brazilian Maritime Authority shows reluctance to implement the nautical bottom concept. They only admit depth measurements obtained from high frequency echo sounders whilst the Manual of Operational Restrictions of the Brazilian Navy defines that seabed with densities greater than 1,200 kg/m³ should not be considered safe for navigation.

In order to implement the nautical bottom concept on a port, it is necessary to provide a thorough research as to convince the reliability of navigating in muddy waterways. Studies must contain a multi-step and integrated approach utilizing geoacoustic and *in situ* measurements (i.e.: density profiling and sediments sampling) and maneuverability tests (Carneiro et al. 2017; McBride et al. 2014; Fontein & Byrd, 2017; Wurpts & Torn, 2005).

The densitometer technique can be led by several devices (i.e.: the tuning fork probe) that have the ability to identify the density gradient within the fluid mud layer through rheological parameters. Such properties can be used to determine the yield strength, which is interpreted as the critical limit where the nautical bottom is defined (Mehta et al. 2014; Teeter 1992; Van Craenenbroeck et al. 1991).

Mud properties can vary considerably from port to port due to different hydrodynamic conditions, material specifications and other features. I.e.: A study developed by IAPH and PIANC (2008) indicates nautical bottom critical densities ranging from 1,150 kg/m³ at Zeebrugge Port in Belgium to 1,270 kg/m³ at Cayenne Port in French Guyana. It is important to develop individual studies and assessment for each port where fluid mud is present and the nautical bottom concept can be implemented.

This research aims at addressing the navigability in fluid mud, sediment silting management and the demands for dredging activities by analyzing the nautical-bottom approach using a combination of various acoustic and *in-situ* measurement techniques. Geoacoustic measurements were obtained at the Port of *Tubarão* (Vitória/Brazil), as seen in Figure 2, using multifrequency acoustic equipment, whereas *in-situ* observations were made through density profiles using the tuning fork technique and sediment sampling.

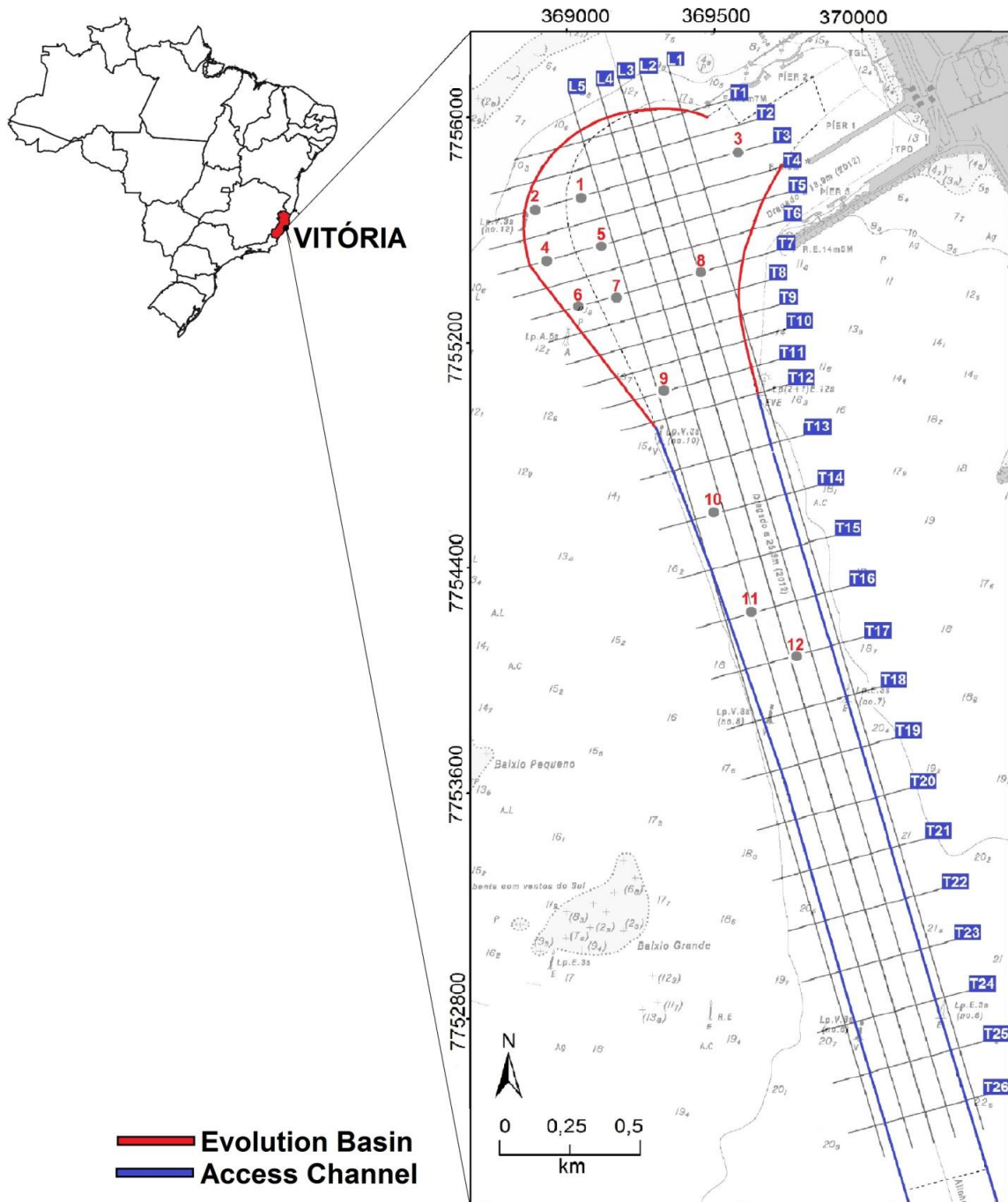


Figure 2 - Location of the Port of *Tubarão*. The evolution basin and the access channel are shown. The surveyed lines are identified in blue boxes and the sediments sampling sites are identified in red.

2. METHODS

Geoacoustic data were surveyed during three days using a multifrequency approach from February 21, 2018. For each line acquisition there are seismic data in the frequency spectrum of 0.5 kHz (Boomer and Sparker), 8-10kHz (low frequency Chirp), 10-20kHz (high frequency chirp), and dual frequency single-beam echo sounder (24,30,33,38/200kHz). This study focuses solely on acoustic data from the SBES and Chirps. 26 transverse and 5 longitudinal transects were surveyed aligned with the navigation channel and evolution basin of the Port of *Tubarão* as seen in Figure 2.

The SBES Kongsberg EA400 (38/200kHz) was used with the Hypack acquisition software. This system has a vertical resolution of 1 cm and accuracy of 1 cm for the higher frequency and 5 cm for the lower frequency. A set of high (HF) and low (LF) frequency Chirps (Meridata Finland) were also used. The MDCS software (Meridata Finland) was used to perform data recording.

The bathymetric data were later loaded onto the Caris HIPS and SIPS and Hypack software for processing, where tide corrections and the elimination of noisy picks were performed. Seismic data were imported the MDPS (Meridata) processing software, where processing (i.e.: noise removal and gain filters) was performed. Results from seismic data interpretation of both SBES and Chirps were used to build thickness maps.

Vessel position and motion were monitored and recorded with a Novatel SE Triple-Frequency GNSS Receiver Position and Orientation System, which consist of two DGPS (Global Positioning System) receivers, using differential corrections.

Instant identification of the mud layer was performed during the survey using the real-time geoaoustic data (38, 200 and 10-20 kHz). Twelve sites were then chosen by pre-identified mud thicknesses and density profiles were performed using the DensiTune® instrument by STEMA (2007) Systems (Figure 4). Thus, two sediment sub-samples (from sites 1 and 12) were collected for the densitometer calibration at locations where the mud seemed to have different acoustical responses.

Sediment samples were also collected at each one of the twelve sites, where the densitometer probe was deployed, using the Van-veen grab sampler. The samples went through laboratory testing for grain-size analysis, organic matter and carbonate content.

The calibration samples were tested for various densities and adjusted to a linear least square trend line. The results were interpolated using the Matlab software, creating a calibration domain of frequency and amplitude per density (Groposo et al., 2014). The calibration domain was applied for editing *in situ* density profiles. Also, the Bingham model was applied for high shear rates (Barnes, 2000; McAnnaly et al., 2007; Mehta et al., 2014; Meshkati et al., 2015), and the calibrated density profiles could be converted into Bingham yield stress profiles (Fonseca, 2018).

As a result of the calibration, it was possible to generate graphics of depth versus density and also an approximation of the Bingham Yield Stress as per function of the subsequent density for the mud containing specific rheological characteristics at the studied port.

Linear correlation was performed considering the depths obtained by the low frequency (38 kHz) single-beam echosounder and the corresponding depths of the various densities. The statistical analysis was performed in order to verify whether the low frequency bathymetric data, which can penetrate through the fluid mud, is associated with the depths values found by the densitometric method for different density levels. The coefficient of determination (R^2), obtained from the linear correlation is a measure of

adjustment of a linear statistical model and it varies from 0 to 1. The closer to 1, the more correlated is the model and the better it fits the sample.

3. RESULTS

The density profiles obtained from the DensiTune tool (Figure 3.a and 3.b) were able to identify the lutocline associated to a sharp step structure in the density profiles. The fluid mud is located within the beginning of the lutocline (lower densities) to the stage where the density is higher than 1200 kg/m³; its actual depth quota is discussed later. Sand and silt content is higher in the sites where the bathymetry and Chirp profiles identified a prominent mud layer (i.e.: samples 1, 4 and 5). Sample 3 showed an almost nonexistent content of fine sediment and the density profile represents the water column density, as the seabed does not contain mud.

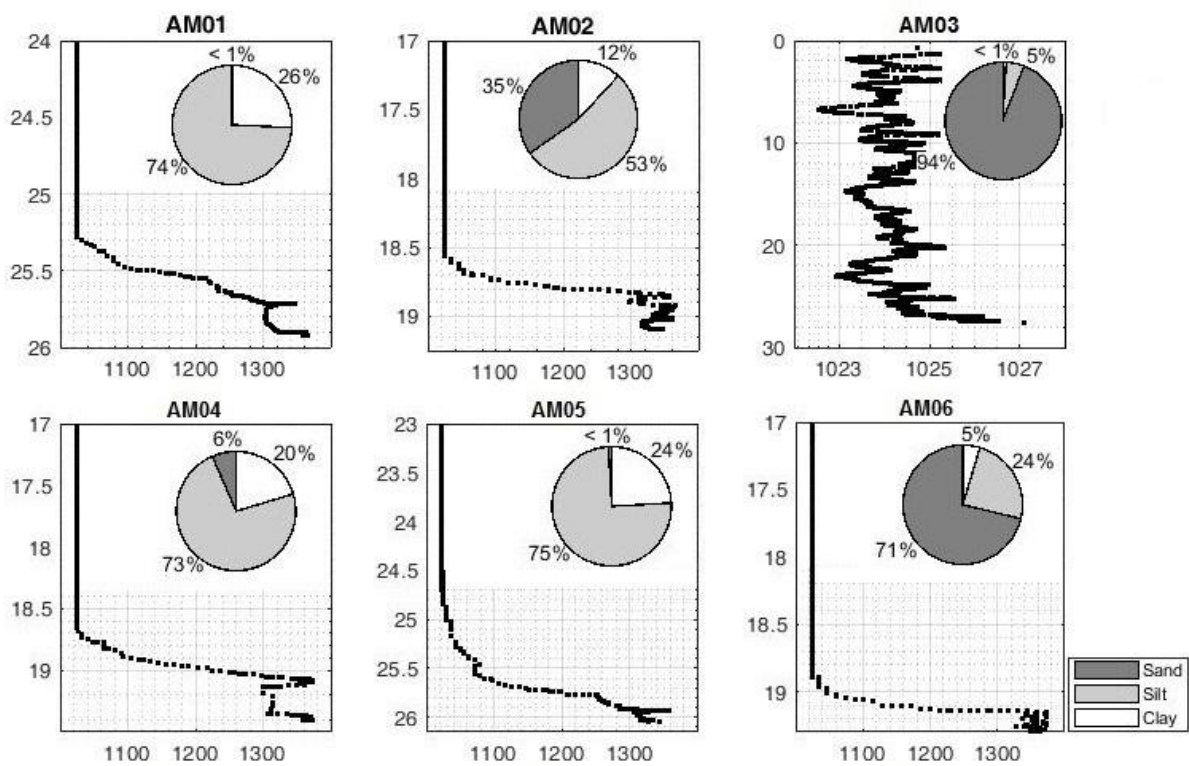


Figure 3.a) - Densitometric profiles (depth versus density) and sediment content (pizza charts) for the twelve surveyed sites (Y axis - m, X axis - kg/m³).

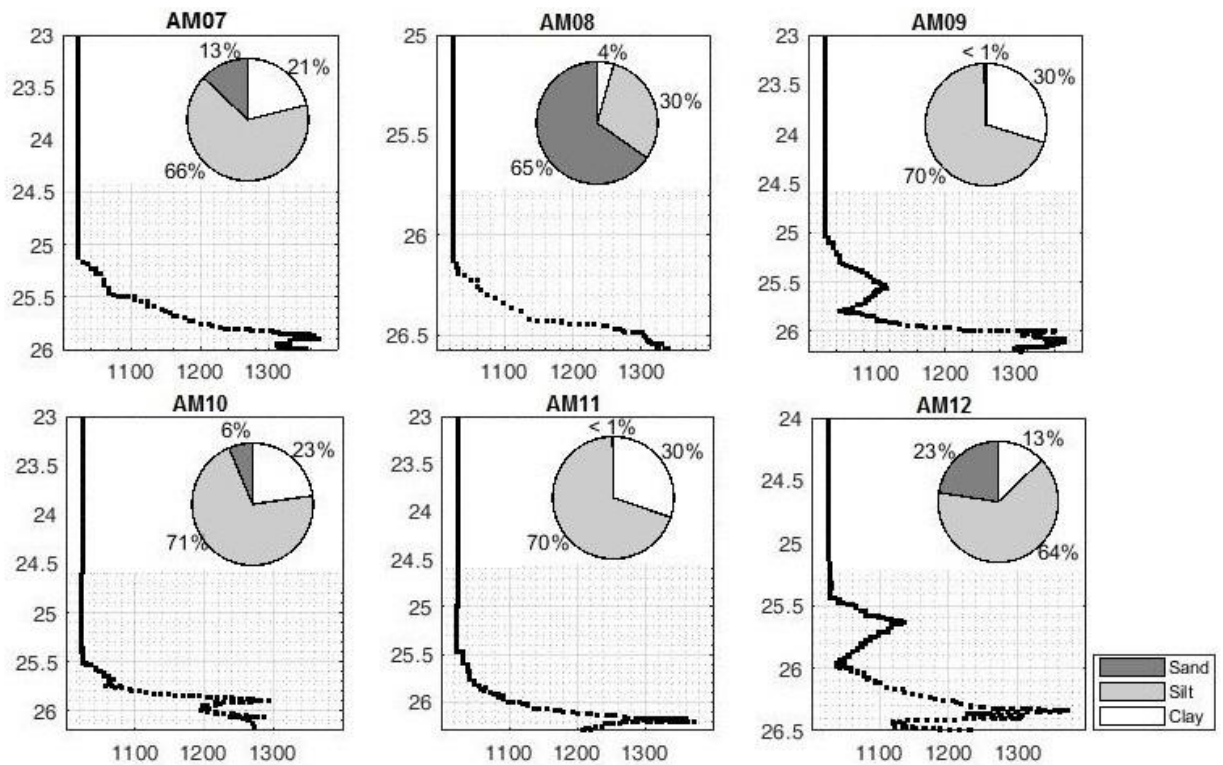


Figure 3.b) - Densitometric profiles (depth versus density) and sediment content (pizza charts) for the twelve surveyed sites (Y axis - m, X axis - kg/m³).

Seismic profiling (Figure 4) obtained with the HF (10-20 kHz) and LF (8-10 kHz) Chirps indicated zones seismically described as reflection-free. The identification of the mud layer was easily seen through Chirp profiles. The acoustic impedance contrast of these different layers is very high, generating a clear pattern with transparent zone, as described by Quaresma (2011), these zones are represented as reflection-free zones.

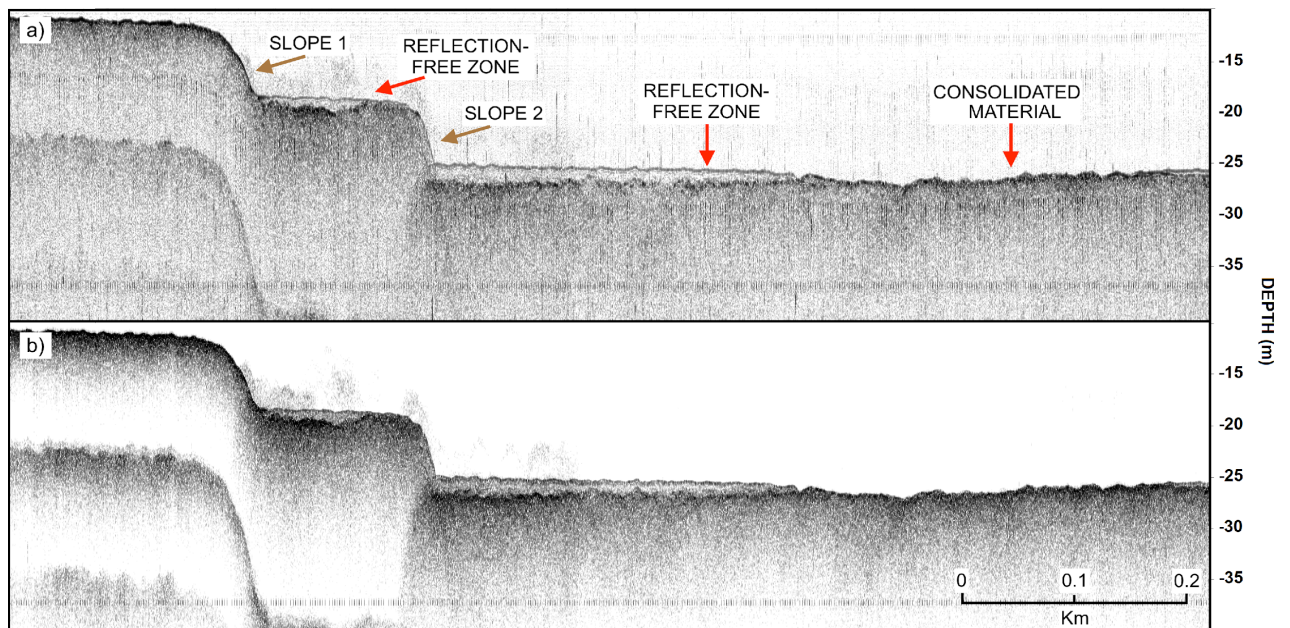


Figure 4 – Chirp data from Transect T4 (evolution basin showing). a) LF (2-10 kHz) profile, b) HF (10-20 kHz) profile. The mud layer is observed while in the middle of the basin no mud is seen.

The seismic acoustic data indicated the presence of fluid mud in the navigation channel and throughout the outer parts of the evolution basin. High spatial variability was found and the fluid mud layer thickness ranged from a few to nearly ninety centimeters. However, there are no reflection-free zones in the central portion of the evolution basin probably associated with resuspension conditions and hydrodynamic transport, generated by the constant passage of large cargo ships (i.e.: the Valemax), also observed during this survey.

The dual frequency SBES data (Figure 5) indicated an anomalous behavior, with heterogeneous centimetric variations of depth between the two frequencies. On both the evolution basin and access channel, it is possible to observe zones with a low reflection pattern (above the yellow lines), possibly related to finer sediments, silt-clay-sized, interpreted as mud. High reflection zones are also seen (above the green lines) with irregular geometry, possibly related to coarser sediments and/or consolidated rocks, such as sandstone or the consolidated clay known as *Tabatinga* (Albino et al., 2006; Bastos et al., 2014).

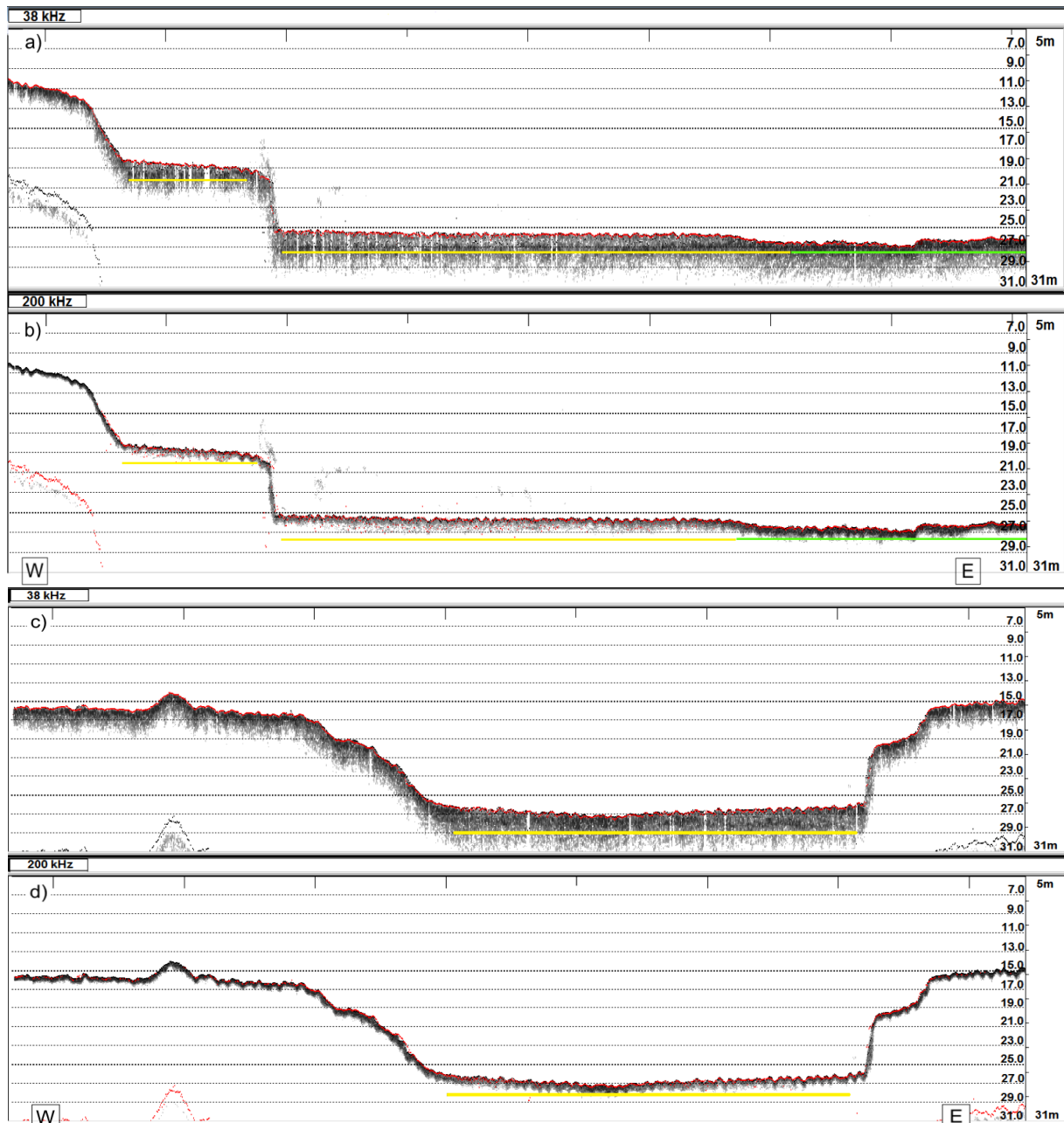


Figure 5 – a) and b) Echograms from transect T3 (evolution basin). c) and d) Echograms from transect T10 (navigation channel). Low reflection zones are seen above the yellow lines, and high reflection zones are seen above green lines.

4. DISCUSSION

The reflection-free zones seen on the Chirp profiles are possibly related to fluid mud going through a consolidation process in which the acoustic impedance contrast is very low within the mud layer, generating such transparent zones. Therefore seismic sources are not capable of identifying the difference between denser and fluid mud, only the contrast between the unconsolidated (sediment in suspension) and consolidated (sandstone or compacted clay) strata. Seismic sources identify only abrupt variations of acoustic impedance (high impedance contrast).

The analysis of SBES records on the Caris Software points to the occurrence of a "double echo" or "displacement" of the reflectors in the areas where fluid mud is present (Figure 6).

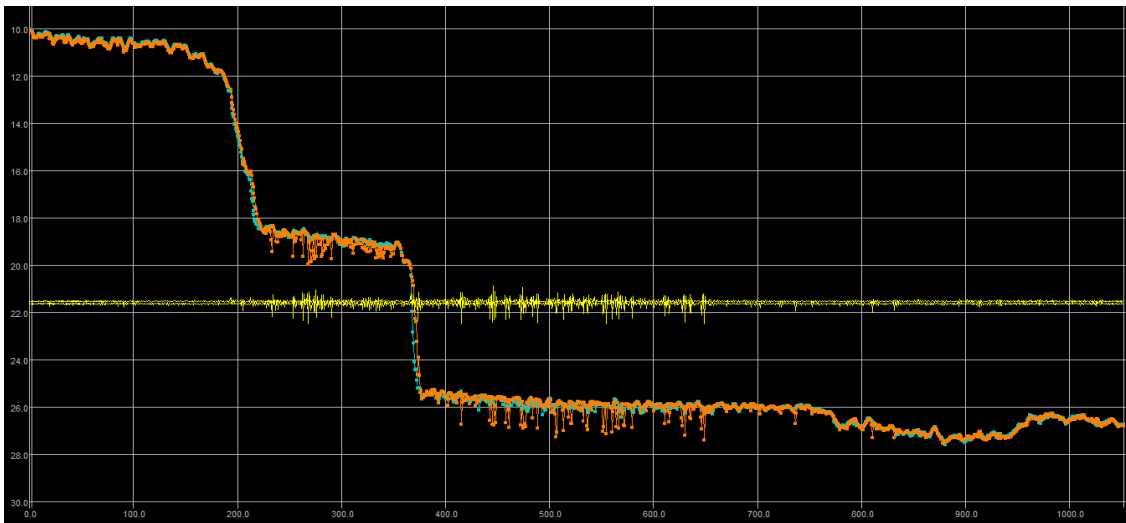


Figure 6 - Single-beam dual frequency echosounder data for transect T4 showing "detachment" (in yellow) from the 38 kHz frequency in orange and the 200 kHz frequency in blue.

The depths obtained by the 200kHz frequency (blue ticks) allow the visualization of the acoustic impedance contrast between the water and the surface of the unconsolidated mud, indicating the density change surface between the water and the lutocline. While the 38kHz frequency (orange ticks) penetrates within the mud and shows the acoustic impedance contrast from a higher density material related to the consolidation process of the fluid mud. That allows the identification of a bottom with lower water content and higher density but not necessarily the consolidated seabed (densities lower than $1,200 \text{ kg/m}^3$), therefore being closer to the real depth values of the lower limit of the fluid mud layer than the higher frequency, therefore this quota can indicate the true seabed depth.

The yellow centered line shows the places where the displacement of the two frequencies happens. It is possible to observe that this phenomenon happens on both slopes where mud was first identified by the Chirp data.

The uncertainty of the accuracy of the depth obtained by the dual frequency bathymetric acoustic method when navigating in a muddy seabed is known by the maritime and port authorities, justifying the lack of trust in using the 38 kHz SBES frequency for determining the seabed depth quota and further implementation of nautical depth (Alexander et al., 1997; PIANC, 2007; Van Leussem & Van Vezem, 1989; Holland et al., 2009).

As demonstrated by Collier & Brown (2005), the fact that the fluid mud is an unconsolidated layer will not necessarily allow the total penetration of the acoustic signal. The displacement of the SBES high and low frequency signals allowed to draw a thickness map of the fluid mud in the light of the density penetration by the echosounder and to compare it with the mud layer thicknesses extracted from the seismic profiles as seen in Figures 7 and 8.

It is possible to compare the thickness maps generated by the detachment of the two SBES frequencies and by the seismic data. Thicknesses from the SBES data is much thinner than the thickness produced from the seismic data due to the limitation of the seismic method to identify only abrupt acoustic impedance contrasts whilst the echosounder is slightly more sensitive to soft acoustic impedance changes. The fluid mud has a gradual and exponential variation of rheological properties (i.e.: density) within its own package, resulting in difficulty for identifying this gradient both by SBES and (specially) by the Chirp (20-50 kHz) source.

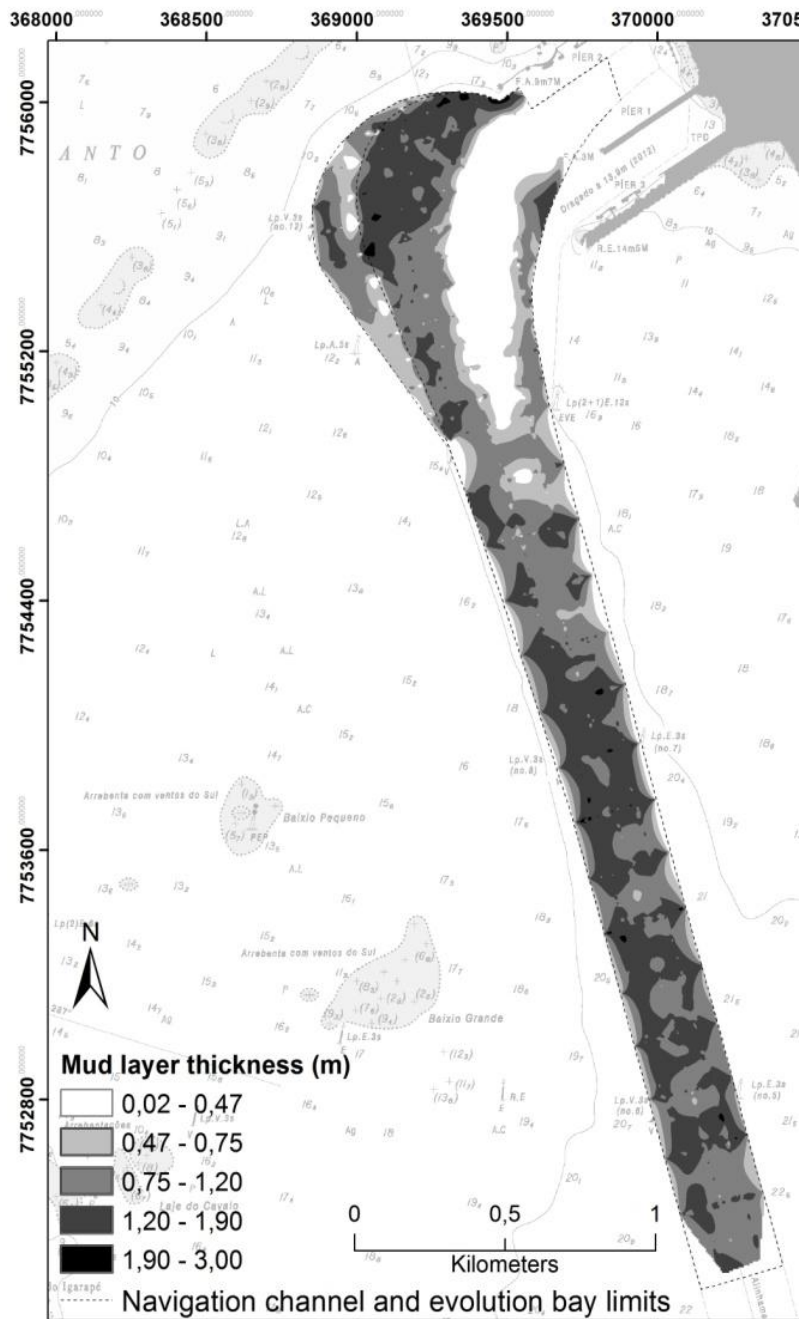


Figure 7 - Mud thickness map from the seismic profiles.

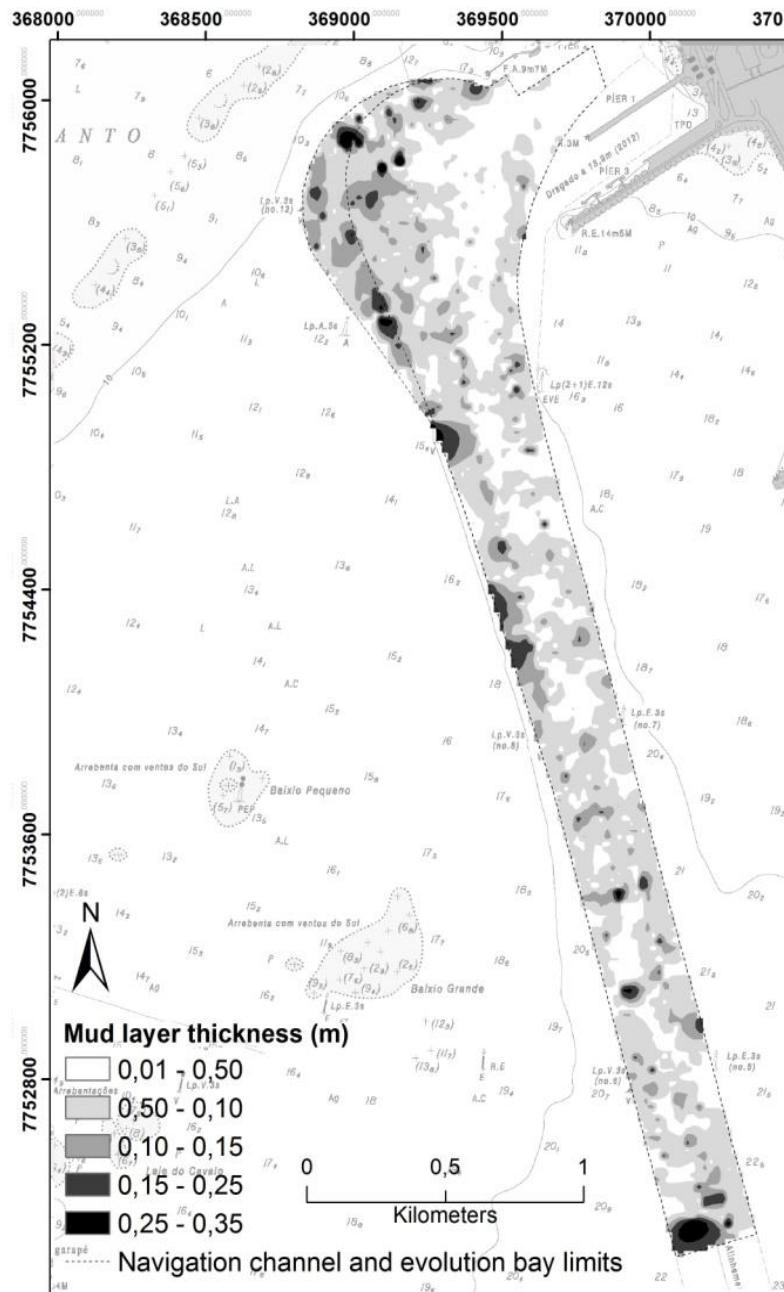


Figure 8 - Mud thickness map from the single beam echosounder profiles.

It is important to notice the lutocline behavior is time-dependent and fluid mud thicknesses can change accordingly to hydrodynamic conditions such as tide, currents and wind velocity (Mehta et al., 2014). Therefore, temporal measurements should also be performed for a better implementation of the nautical bottom concept.

Another important feature when dealing with navigating in fluid mud is the content of sand, as some studies indicate that sand reduces the yield stress (Granboulan et al., 1989; Van Craenenbroeck et al., 1991; Wurpts and Torn, 2005). Sample 1 (with 0.17% sand content) shows a higher yield stress than sample 12 (with 22% sand content) as observed in Figure 9. The chart with Bingham yield stress versus density helps determine the critical values where density inflection happens and nautical bottom can be determined within an acceptable yield stress range without presenting risks for ships navigation.

Sample 3, 6 and 8 (with 94, 71 and 65 % sand content) seems to have followed the same pattern.

The transition of pseudo-plastic liquid to plastic liquid mud is observed at a very distinct bending point in the tuning fork response, this point marks the density where the mud can be characterized by a significant yield-strength value. The rheological transition from a smooth to an abrupt yield stress versus the density curve marks the critical value of density (McBride, 2014).

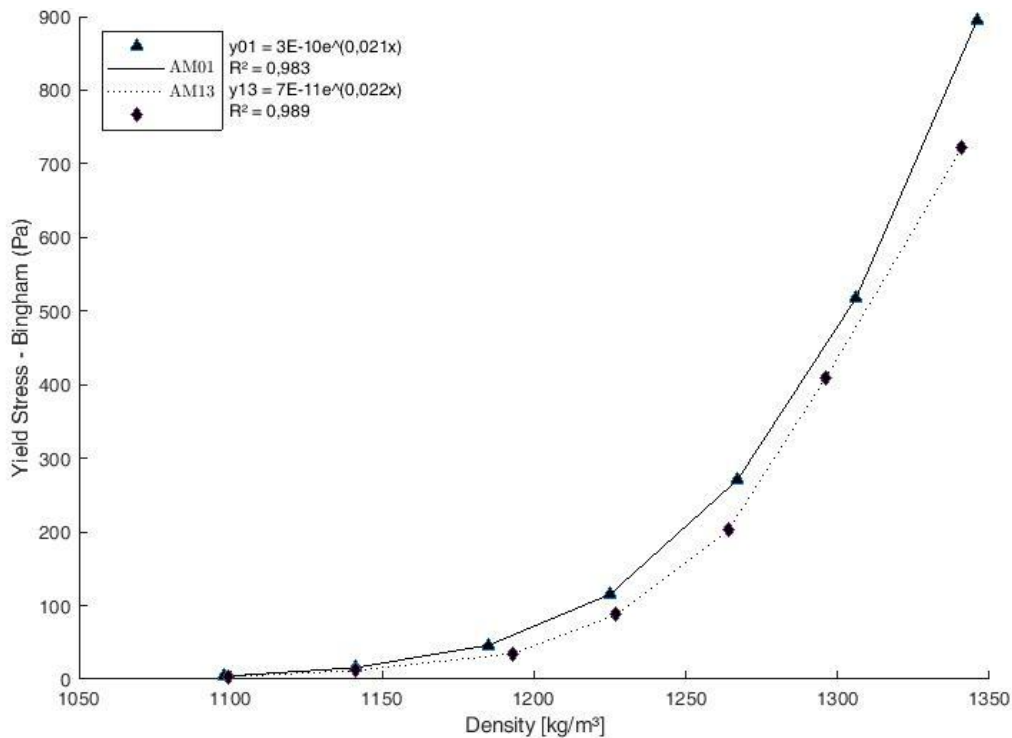


Figure 9 - Bingham yield stress versus density for the two tested calibration samples. The exponential trend adjustments are shown.

In this approach, critical density values at approximately 1.150 and 1.175 kg/m³ would be associated with Samples 1 and 12, respectively. Considering the top of the fluid mud layer as the inflection point of the lutocline (1.100 kg/m³), where the water density values change abruptly, and the bottom of this layer is the same as the depth found for the critical density values, corresponding to the critical Bingham yield point of 50Pa. In the light of this information, a layer of potentially navigable fluid mud is observed, with the highest thickness values available in the navigation channel (Sample 13) and the lowest in the evolution basin (Sample 1). The 50 Pa value associated with the critical density comes from several studies that point out the rheological values in which navigation is still safe.

The results concerning the linear correlation performed between the depths obtained in the low frequency echo sounding (38 kHz) and the depths corresponding to the densities of 1150, 1175, 1200, 1225, 1250 kg/m³ obtained by the DensiTune method are presented in the following table. It is possible to observe that the best values of the coefficient of correlation (R^2) were found in the correlation between the depths obtained

with the low frequency echo soundings and the depth at which the specific masses of 1150 and 1175 kg/m³ occur (Table 1).

| Correlation - Volumetric Mass Density x Bathymetry | | | | | |
|--|--------|--------|--------|--------|--------|
| Density (Kg/m ³) | 1150 | 1175 | 1200 | 1225 | 1250 |
| R ² | 0,7854 | 0,8145 | 0,7631 | 0,4249 | 0,1579 |

Table 1 - R² obtained by the linear correlation between the depths found for the SBES 33kHz frequency and the corresponding depths for the volumetric mass density of 1150, 1175, 1200, 1225, 1250 kg/m³.

Considering the results above, the layer of fluid mud has thicknesses ranging from 0,18 to 0,90 cm, whereas at the sampling site 3 no fluid mud was observed and the density profile indicated the water column.

Through the determination of the density values the acoustic signal of the 200 kHz frequency echosounder recognized as the seabed a depth with a minimum density of 1,100 kg/m³ and the frequency of 38 kHz would be associated with densities ranging from 1150 to 1,200 kg/m³, related to 50 Pa Bingham yield stress.

A particular value of rheological mud properties (i.e.: yield stress) is used in some other cases to define the criteria for the navigation in fluid mud. At the Port of Edem, in Germany, the navigable depth reference is defined adopting 100Pa as the critical yield stress value. In the case of the Port of *Tubarão*, if this criterion is to be considered, the corresponding critical densities would vary from 1,230 to 1,240 kg/m³. Considering this criterion, in the presented measurements, potentially navigable layers from 30 to 95 cm could be envisioned for safe navigation.

Similar results were found at the Port of Zeebrugge in Belgium. The analyzed mud showed comparable Bingham yield stress for samples less than 1,200 kg/m³ Meshkati et al. (2015). Nevertheless, there was a significant increase in the yield stress at approximately 1,200 kg/m³, which was observed for the *Tubarão* samples only at 1,150 kg/m³ for both the calibration samples 1 and 13. Same behavior for Zeebrugge mud was also reported (Van Craenenbroeck et al., 1991), where yield stress values for low sand content samples increased abruptly at 1,150 kg/m³.

5. CONCLUSION

Chirp profiles cannot help conclude whether mud layers represent positively only fluid mud. This equipment identifies abrupt variations of acoustic impedance whilst within the fluid mud package there are smooth variations of density.

The low-frequency (38kHz) data does not necessarily represent the actual bottom of the fluid mud layer as it is constituted by densities lower than that indicated by the Navy's Manual of Operational Restrictions (1,200 kg/m³). Insofar the high frequency data (200 kHz) identified the top of the fluid mud layer as the consolidated seabed although this layer has densities even lower (1050 kg/m³) than that indicated for safe navigation.

The densities of 1150 and 1200 kg/m³ obtained the best volumetric mass density correlation with the bathymetric surveys of 38 kHz, being those, the density values that

most should approach the reference critical density for the definition of the nautical bottom for the Port of *Tubarão*. These values are very close to reference densities used worldwide in port areas with muddy bottoms. Such frequency showed a reasonable approximation to the actual depth of the fluid mud layer, identified by the densitometer, although it is not responsive to subtle rheological aspects within the mud layer. Therefore, the identification of the nautical depth should not be relied on bathymetric acoustic methods only, such as the SBES but also on *in-situ* data, such as the densitometer.

It was observed that a critical density ranging from 1150 to 1,200 kg/m³ could be adopted, if the critical yield stress of 50 Pa is considered. However, greater values of up to 1240 kg/m³ could be used, if the value of 100Pa for yield stress is to be considered. Therefore, potentially navigable layers ranging from a few centimeters up to 95 cm could be adopted.

The Port of *Tubarão* can benefit from this methodology as it can be used in the analysis and identification of areas with fluid mud for management of sediments silting, navigating in muddy areas and for the improvement of dredging activities. It is important that the use of the nautical bottom concept relies not only on rheological aspects but also on multidisciplinary research.

In a scenario of increase in the draft of the ships and navigation in fluid mud, the concept of nautical depth assessed by this approach presents itself as an economically attractive possibility.

6. REFERENCES

- Albino, J.; Girardi, G.; Nascimento, K. A. 2006. *Erosão e Progradação do litoral do Espírito Santo*. In: Muehe, D. (Org.). *Erosão e Progradação do Litoral do Brasil*. Brasília: Ministério de Meio Ambiente, v. 1:226-264.
- Alexander, M.P.; Teeter, A.M.; Banks G.E. 1997. Development and verification of an intrusive hydrographic survey system for fluid mud channels. Tech. Rep. No. DRP-97-1,U.S. Army Engineer Waterways Experiment Station, Vicksburg, Miss.
- Bastos, A. C.; Costa Moscon, D. M.; Carmo, D.; Baptista Neto, J. A.; Quaresma, V.S. 2014. Modern sedimentation processes in a wave-dominated coastal embayment: Espírito Santo Bay, southeast Brazil. *Geo-Marine Letters* , v. 35, p. 23-36.
- Barnes, H. A. 2000. A handbook of elementary rheology, Univ. of Wales– Institute of Non-Newtonian Fluid Mechanics, Aberystwyth, U. K.
- Buchanan, L. 2005. Difficulties of surveying in fluid mud, the effects of bathymetry of suspended sediments in the water column. *Hydro-International*, Volume 9, Number 6.
- Carneiro, J.C.; Fonseca, D.L.; Vinzon, S.B.; Gallo, M.N. 2017. Strategies for measuring fluid mud layers and their rheological properties in ports. *J. Waterway Port Coastal Ocean Eng* 143:04017008. [https://doi.org/10.1061/\(ASCE\)WW.1943-5460.0000396](https://doi.org/10.1061/(ASCE)WW.1943-5460.0000396)
- Clayes, S. 2006. Evaluation and combination of techniques used to determine the Nautical Bottom - A call for rheology based instruments. *Evolutions in hydrography*. Antuerpia, Belgium. p. 141-144
- Collier, J.S.; Brown C.J. 2005. Correlation of sidescan backscatter with grain size distribution of surficial seabed sediments. *Marine Geology*, 214: 431–449.
- Dyer, K.R. 1986. *Coastal and estuarine sediment dynamics*. Chichester UK, John Wiley & Sons, 342 p.

- Fonseca, D.L.; Cunha P.M.; Carneiro, J.; Gallo, M., Vinzón, S.B. 2018. Assessing rheological properties of fluid mud samples through tuning fork data. *Ocean Dynamics*.
- Fontein, W.F.; Byrd, R.W. 2007. The nautical depth approach, a review for implementation. In: WODCON XVIII ANNUAL DREDGING SEMINAR. WEDA
- Granboulan, J.; Feral, A.; Villerot, M.; Jouanneau, J. M. 1989. Study of the sedimentological and rheological properties of fluid mud in the fluvio-estuarine system of the Gironde estuary. *Ocean Shore. Manage.*, 12(1), 23–46.
- Groppo, V.; Mosquera, R.L.; Pedocchi, F.; Vinzón, S.B.; Gallo, M. 2014. Mud density prospection using a tuning fork. *JWaterw Port Coast Ocean Eng* 141:04014047. [https://doi.org/10.1061/\(ASCE\)WW.1943-5460.0000289](https://doi.org/10.1061/(ASCE)WW.1943-5460.0000289)
- Holland T.K.; Vinzon, S.B.; Calliarl, L.J. 2009. A field study of coastal dynamics on a muddy coast offshore of Cassino Beach, Brazil. *Continental Shelf Research* 29: 503–514.
- Kineke, G. C.; Sternberg, R. W. 1995. Distribution of fluid muds on the Amazon continental shelf. *International Journal of Marine Geology, Geochemistry and Geophysics*, n. 125, p. 193-233.
- Kirby, R.; Parker, W.; Van Oostrum, W. 1980. Definition of the seabed in navigation routes through mud areas. *International Hydrographic Review*, Vol. XVII (1). pp. 107-117.
- Kirichek, A.; Chassagne C.; Winterwerp H.; Noordijk A.; Rutgers R.; Schot, C.; Nipius, K.; Vellinga, T. 2018. How Navigable Are Fluid Mud Layers. *PIANC-World Congress Panama City, Panama*.
- Madson, J.; Sommerfield, C. K. 2003. Application of sidescan sonar, sub bottom profiling and echo sounding techniques to study sediment deposition and erosion in estuaries: Results from the lower Delaware River and upper Delaware Bay. *Proc., US Hydro Conf.*, 24–27.
- McAnally, W.H., F.ASCE; Friedrichs, C.; Hamilton, H.; Hayter, E.; Shrestha, P.; Rodriguez, H.; Sheremet, A.; Teeter, T. ASCE. 2007a. Management of Fluid Mud in Estuaries, Bays and Lakes. I: Present State of Understanding on Character and Behavior. Task Committee on Management of Fluid Mud.
- McAnally, W.H., F.ASCE; Teeter, A.; Schoellhamer, D.; Friedrichs, C.; Hamilton, D.; Hayter, E.; Shrestha, P.; Rodriguez, H.; Sheremet, A.; Kirby, K. ASCE. 2007b. Management of Fluid Mud in Estuaries, Bays and Lakes. II: Measurement, Modeling, and Management. Task Committee on Management of Fluid Mud.
- Mehta, A.J.; Hayter, E.J.; Parker, W.R.; Tester, A.M. 1987. Cohesive sediment transport processes. in: Sedimentation control to reduce maintenance dredging of navigation facilities in estuaries. Report and symposium proceeding. National Academic Press, Washington, D.C., 1987. p.53-76.
- Mehta A. J.; Dyer, K. 1990. Cohesive sediment transport in estuarine and coastal waters. In: LE MEHAUTE B & HANES DM (Eds.). *The sea: ideas and observations on progress in the study of the seas*. New York, Wiley-Interscience, 9, Part B, p. 815–839.
- Mehta A. J.; M.ASCE; Samsami F.; Yogesh P.; Sahin, C. 2014. Fluid Mud Properties in Nautical Depth Estimation. *Journal of Waterway, Port, Coastal, and Ocean Engineering*, n. 140, p. 210-222.
- Meshkati, M. E.; Claeys, S.; Van Hoestenbergh, T.; Staelens, P.; Van Oyen, T.; Vanlede, J.; De Sutter, R. 2015. The effect of different physico-chemical parameters on the rheological behavior of consolidating mud. *Proc., 13th Int. Conf. on Cohesive Sediments*, E. Toorman, T. Mertens, M. Fettweis, and J. Vanlede, eds., Flanders Marine Institute, Oostende, Belgium, 193–194.
- McBride, M. 2014. Harbour approach channels—Design guidelines. *PIANC Report No. 121*. World Association for Waterborne Transport Infrastructure, Brussels, Belgium
- Nederlof, L. 1978. “Varen boven slib” in het Rotterdamse haven-en rivieren-gebied. *Gementewerken Rotterdam*. 98.21-R7332.
- Noernberg, M. & Soares R.C., (2007). *A presença de lama fluida navegabilidade no canal de acesso à região portuária de Antonina (PR)*. 49° *Geology Brazilian Congress*. August 2018 – Rio de Janeiro.

- Parker, W.R. Lee, K. 1979. The behavior of fine sediment relevant to the dispersal of pollutants. In: ICESWorkshop on Sediment and Pollutant Interchange in Shallow Seas. p. 28–34.
- Quaresma, V.S.; Bastos, A.C.; Loureiro, D.V.; Paixão, S. 2011. *Utilização de métodos geofísicos para mapeamento de lama fluida no porto de tubarão, Vitória (ES-Brasil)*. *Revista Brasileira de Geofísica*. 29(3): 487-496.
- PIANC. 2008. Minimising harbour siltation. Report no 102, p 75
- PIANC. 2014. Harbour Approach Channels - Design Guidelines, Report 121, PIANC, Brussels.
- Schettini, C. A. F.; Almeida, D. C.; Siegle, E.; Alencar, A. C. B. 2010. A snapshot of suspended sediment and fluid mud occurrence in a mixed-energy embayment, Tijucas Bay, Brazil. *Geo-Mar Lett.*, 30(1), 47–62.
- Schrottke, K.; Becker, M.; Bartholomä, A.; Flemming, B. W.; Hebbeln, D. 2006. Fluid mud dynamics in the Weser estuary turbidity zone tracked by high-resolution side-scan sonar and parametric sub-bottom profiler. *Geo-Marine Lett.*, 26(3), 185–198.
- Shi, Z.; Ren, I. F.; Hamilton, I. J. 1999. “Acoustic profiling of fine suspension concentration in the Changjiang estuary.” *Estuaries*, 22(3), 648–656.
- Sills, G.C. 1994. Hindered settling and consolidation in cohesive sediments. In: 4th Nearshore and Estuarine Cohesive Sediment Transport Conference INTERCOH 94, Wallingford – England, Paper 10.
- STEMA 2007 DensiTune® User’s Manual - Version 4.2. STEMA Survey Services. The Netherlands.
- Teeter, A. M. 1992. *Evaluation of new fluid mud survey system at field sites*. Dredging Research Technical Note DRP-92-5. Vicksburg, MS: U.S. Army Engineer Research and Development Center
- US Army Corps of Engineers, (2002), “Depth Measurement Over Irregular or Unconsolidated Bottoms”, Engineering Manual 1110-2-1003, Chapter 21, Department of the Army, Washington, DC.
- USACE. 2013. Depth measurement over irregular or unconsolidated bottoms. In *Engineer Manual, Hydrographic Surveying*, Ch. 21, EM 1110-2-1003. Washington, DC: U.S. Army Corps of Engineers.
- Van Craenenbroeck, K.; Vantorre, M.; De Wolf, P. 1991. “Navigation in muddy areas—Establishing the navigable depth in the Port of Zeebrugge.” *Proc.*, CEDA-PIANC Conf.
- Van leussen, W.; Van Velzen, E. 1989. High concentration suspensions: their origin and importance in Dutch estuaries and coastal waters. *Journal of Coastal Research*, SI 5: 1–22.
- Welp, T.L. and Tubman, M.W. 2017. Present Practice of Using Nautical Depth to Manage Navigation Channels in the Presence of Fluid Mud) Technical Report. U.S. Army Corps of Engineers Vicksburg United States
- Whitehouse, R.; Soulsby, R.; Roberts, W.; Mitchener, H. 2000. Dynamics of estuarine muds. HR Wallingford, London, 210 p.
- Wolanski, E.; Gibbs, R. J.; Mazda, Y.; Metha, A.; King, B. 1992. “The role of turbulence in the settling of mud flocs.” *J. Coastal Res.*, 8(1), 35–46.
- Wurpts, R. 1998. The question of definition of the nautical depth in fluid mud by aid of rheological properties. *Proceedings of the 15 th World Dredging Congress, Las Vegas, Nevada, USA*.
- Wurpts, R.; Torn, P. 2005. 15 years’ experience with fluid mud: Definition of the nautical bottom with rheological parameters. *Terra et Aqua*, 99(Jun), 22–32.

CHAPTER 6

FINAL CONSIDERATIONS

For exploration and monitoring projects of port environments, products that allow an approach both from the point of view of resolution and penetration are required. Currently there is a wide range of geoacoustic equipment capable of obtaining the most varied results according to their different frequencies. Thus, to understand and compare the acoustic responses of each of these frequencies is fundamental for determining their usage in ports. The application of these equipment and frequencies is of great relevance for the port sector and this dissertation approached and discussed this issue in the light of different aspects, divided into the following chapters.

Chapter two showed comparisons between the seismic frequencies as a function of their penetration and resolution capacities. The identification of the thicknesses of the geological layers in subsurface was measured and it was observed that the thicknesses of the shallow sedimentary layers are directly related to the frequency emitted by the seismic sources and petrophysical characteristics of the strata such as mean grain size and density. This chapter assists in the production of information on volume calculations for dredging activities, such as volume of silted material, depth of the rocky basement and geohazards. Special attention should be given to regions with presence of fluid mud, where seismic geoacoustic equipment is not necessarily suitable for volume calculations.

Chapter three covered navigation on fluid mud, known as nautical depth approach, through the use of the singlebeam echosounder, tuning fork technique, *in-situ* sediment particle size analysis and rheological properties. The combination of the mentioned techniques proved to be more suitable for navigation assessment considering the nautical bottom approach rather than the use of only acoustic methods. Considering solutions already used in the largest ports in the world, studies on fluid mud might lead to dredging reductions and draft increases.

The subjects presented in this dissertation allow to conclude on the importance of the simultaneous use of multifrequency systems in the investigation of submerged environments of port areas, aiming at a complete geological and geotechnical approach of the surface and subsurface of the investigated area. The use of a whole data set of seismics (chirps, boomers and sparkers), bathymetry (single and multibeam echosounders) and *in-situ* data (densitometric profiling and sediment sampling) sum up the ideal approach for mapping and evaluating the surface and subsurface of port areas, therefore leading to a better determination of the nautical depth and navigation risks assets.

Activities such as dredging, geohazards monitoring and nautical depth assessment can be achieved and their costs minimized, leveraging the production and capacity of a port.